Toxicology Reports 8 (2021) 846–862

Contents lists available at ScienceDirect

Toxicology Reports

journal homepage: www.elsevier.com/locate/toxrep

Vehicle emissions-exposure alters expression of systemic and tissue-specific components of the renin-angiotensin system and promotes outcomes associated with cardiovascular disease and obesity in wild-type C57BL/6 male mice

Benjamin L. Phipps, Usa Suwannasual, JoAnn Lucero, Nicholas A. Mitchell, Amie K. Lund *

Advanced Environmental Research Institute, Department of Biological Sciences, University of North Texas, Denton, TX, 76201, USA

ARTICLE INFO

Edited by Dr. A.M Tsatsaka

Keywords:
Air pollution
Renin-angiotensin system
Obesity
Adipose
CVD

ABSTRACT

Exposure to air pollution from traffic-generated sources is known to contribute to the etiology of inflammatory diseases, including cardiovascular disease (CVD) and obesity; however, the signaling pathways involved are still under investigation. Dysregulation of the renin-angiotensin system (RAS) can contribute to CVD and alter lipid storage and inflammation in adipose tissue. Our previous exposure studies revealed that traffic-generated emissions increase RAS signaling, further exacerbated by a high-fat diet. Thus, we investigated the hypothesis that exposure to engine emissions increases systemic and local adipocyte RAS signaling, promoting the expression of factors involved in CVD and obesity. Male C57BL/6 mice (6–8 wk old) were fed either a high-fat (HF, n = 16) or low-fat (LF, n = 16) diet, beginning 30d prior to exposures, and then exposed via inhalation to either filtered air (FA, controls) or a mixture of diesel engine + gasoline engine vehicle emissions (MVE: 100 μg PM/m^3) via whole-body inhalation for 6 h/d, 7 d/wk, 30d. Endpoints were assessed via immunofluorescence and RT-qPCR. MVE-exposure promoted vascular adhesion factors (VCAM-1, ICAM-1) expression, monocyte/macrophage sequestration, and oxidative stress in the vasculature, associated with increased angiotensin II receptor type 1 (AT1) expression. In the kidney, MVE-exposure promoted the expression of renin, AT1, and AT2 receptors. In adipose tissue, both HF-diet and MVE-exposure mediated increased epididymal fat pad weight and adipocyte hypertrophy, associated with increased angiotensinogen and AT1 receptor expression; however, these outcomes were further exacerbated in the MVE + HF group. MVE-exposure also induced inflammation, monocyte chemoattractant protein (MCP)-1, and leptin, while reducing insulin receptor and glucose transporter, GLUT4, expression in adipose tissue. Our results indicate that MVE-exposure promotes systemic and local adipose RAS signaling, associated with increased expression of factors contributing to CVD and obesity, further exacerbated by HF diet consumption.

1. Introduction

Exposure to air pollution is estimated to contribute to over 7 million deaths worldwide annually [1]. Several studies have established that exposure to traffic-generated air pollutants contributes to the etiology, or exacerbation, of multiple diseases, including cardiovascular disease (CVD) (rev. in [2,3]. Heart disease is the leading cause of death in the U. S.; atherosclerosis is the primary contributor to heart attack and stroke [4]. Atherosclerosis vascular disease is characterized by inflammation and plaque deposition in the vessel wall, resulting from increased

Abbreviations: ACE, angiotensin converting enzyme; AGT, angiotensinogen; Ang II, angiotensin II; AT1, angiotensin II receptor subtype 1; AT2, angiotensin II receptor subtype 2; CVD, cardiovascular disease; DHE, dihydroethidium; FA, filtered air (controls); GLUT-4, glucose transporter type 4; ICAM-1, intracellular adhesion molecule-1; IL-6, interleukin-6; IL-β, interleukin beta; IR, insulin receptor; LDL, low density lipoprotein; LF, low-fat diet; HF, high-fat diet; LOX-1, lectin-like oxidized low-density lipoprotein receptor; MCP-1, monocyte chemoattractant protein-1; MOMA-2, anti-monocyte + macrophage antibody; MVE, mixed gasoline and diesel vehicle emissions; PM, particulate matter; RAS, renin-angiotensin system; ROS, reactive oxygen species; TNF-α, tumor necrosis factor alpha; T2D, type 2 diabetes; VCAM-1, vascular cell adhesion molecule-1; vWF, Von Willebrand factor.

* Corresponding author at: University of North Texas, 1704 W. Mulberry – EESAT Building, Rm #215, Denton, TX, 76201, USA.
E-mail address: amie.lund@unt.edu (A.K. Lund).

https://doi.org/10.1016/j.toxrep.2021.04.001
Received 14 January 2021; Received in revised form 3 April 2021; Accepted 9 April 2021

low-density lipoprotein (LDL) cholesterol and monocyte/macrophage infiltration. Increased expression of intercellular adhesion molecule (ICAM) -1 and vascular cell adhesion molecule (VCAM)-1, which promote the adhesion of leukocytes to the vascular wall, is thought to be one of the initial cellular responses involved in the pathogenesis of atherosclerotic lesions [5,6]. Increased inflammatory signaling and reactive oxygen species (ROS) production are also primary contributors to atherogenesis [7].

CVD is closely associated with several other inflammatory-mediated disease states, including type 2 diabetes (T2D) and obesity [8]. The high-fat "Western" diet, which is rich in carbohydrates and saturated fats, is a well-characterized player in these co-morbidities (rev. in [9, 10]. Environmental air pollution is another such factor, and while the composition of air pollution varies significantly between regions, several ubiquitous components are implicated in disease. Exposure to both particulate matter (PM) and complex mixtures, including that derived from vehicle emissions, have been implicated in CVD and cardiometabolic disease states [11–14]. Recent studies have also established a link between exposure to air pollution and obesity [15,16]. Furthermore, exposure to ambient air pollution has been shown to promote inflammation, oxidative stress, and dyslipidemia, associated with metabolic dysfunction and weight gain in animal models [17].

While previous studies have implicated air pollution in various cardiovascular and cardiometabolic disease states, the molecular mechanisms by which these pollutants mediate these comorbidities have not been fully elucidated. Dysregulation of the renin-angiotensin system (RAS) may be one potential mechanism. The RAS functions through the conversion of angiotensinogen (AGT), produced primarily in the liver. Renin, produced by the kidneys, then converts AGT to angiotensin I (Ang I), which is processed by the angiotensin-converting enzyme (ACE) to cleave the active peptide, Ang II [18]. Ang II's physiologic effects are primarily mediated by signaling through either the AT1 or AT2 receptor types [19]. Ang II -AT1 signaling is also known to activate NADPH oxidases, involved in ROS formation [20]. Increased systemic RAS signaling has been well characterized to promote CVD, with both ACE-inhibitor and AT1 antagonist pharmacotherapies beneficial in treating hypertension and other CVDs [21]. Moreover, a recent study reports that exposure to $PM_{2.5}$ resulted in elevated blood pressure associated with increased systemic Ang II and AT1 receptor expression in the vasculature and kidney, which was further exacerbated in offspring with parental $PM_{2.5}$ exposures [22].

In addition to the systemic RAS described above, certain tissue types, including adipose tissue, possess a localized RAS [23]. AGT produced in the adipose tissue is believed to be a key source of AGT measured in the systemic circulation, with elevated AGT often observed in obese patients [24,25]. The RAS is also proposed to promote adipocyte growth and cellular differentiation, which is evidenced through studies that show that the upregulation of RAS components positively correlates with adipose mass [26–29]. AT1 antagonist-treatment has been shown to limit weight gain in high-fat (HF) diet-fed rodent studies [30]. Moreover, blockade of the AT1 receptor has been reported to reduce adipocyte size, adipose tissue weight, and inflammation in both atherosclerotic and diabetic mouse models [31]. Ang II has also been reported to interfere with skeletal muscle glucose transport through impairing glucose transporter (GLUT)-4 translocation [32], which can lead to insulin resistance [33]. Both insulin and tumor necrosis factor (TNF)-α have been reported to regulate adipocyte AGT expression [34–36], and TNF-α has been identified as a contributor to obesity [37]. Furthermore, Ang II has been demonstrated to induce inflammatory signaling in adipose tissue, including expression of monocyte chemoattractant protein (MCP)-1 and interleukins (IL), such as IL-6 [38,39].

While more recent interest in air pollution and RAS signaling has emerged because of the reported association between air pollution exposure and COVID-19 (SARS-CoV-2) susceptibility in the lungs [40, 41], and associated cardiovascular effects [42,43]; there are still significant gaps in knowledge related to how air pollution alters systemic and adipose tissue-specific RAS signaling and how this may promote CVD and metabolic syndrome or obesity. Understanding key mechanistic pathways by which traffic-generated air pollution exposure can promote inflammatory comorbid disease states such as CVD, metabolic syndrome, and obesity is necessary for preventative and therapeutic targets, and also environmental regulatory outcomes. Our laboratory has reported that inhalation exposure to a ubiquitous source of ambient air pollution, namely a mixture of diesel and gasoline vehicle engine exhaust (MVE), leads to elevated systemic Ang II plasma levels, associated with increased cerebrovascular expression of the AT1 receptor in C57BL/6 wild-type mice, which were further elevated in HF-diet fed animals [44]. These findings suggest that exposure to traffic-generated pollutants may alter RAS signaling. Therefore, in the current studies, we investigated whether MVE-inhalation exposure ± a HF diet promotes systemic and local adipocyte RAS signaling, contributing to the expression of factors involved in the pathogenesis of CVD and promotion of obesity.

2. Methods

2.1. Mixed vehicle emissions inhalation exposure protocol

Male 6–8 week-old C57BL/6 mice (C57BL/6NTac, Taconic, Albany, NY) were fed either a low-fat (LF) standard chow or high-fat diet (HF: TD88137 Custom Research Diet, Harlan Teklad, Madison, WI; 42 % kcal from fat, 21.2 % fat content by weight) for 30 d. Mice on each diet were then randomly sorted to be exposed by inhalation to either a combined mixture of diesel engine and gasoline engine vehicle emissions (MVE: 70 μg PM/m^3 diesel engine exhaust + 30 μg PM/m^3 gasoline engine exhaust, n = 16; n = 8 HF diet, n = 8 LF diet) or filtered-air (FA: controls, n = 16; n = 8 HF diet, n = 8 LF diet) for 6 h/d, 7 d/wk, for 30 d. As previously detailed by our laboratory, the MVE was generated by combining the emissions from a Yanmar diesel generator system with those from a 1996 GM gasoline engine [45]. The resulting mixture was characterized daily for chemical composition throughout the exposures, as previously detailed (Lund et al. 2011; [44]). While higher than average PM concentrations rates, 100 μg PM/m^3 is within the daily levels of $PM_{2.5}$ measured across heavily populated urban areas, as well as certain occupational settings [46,47,48]. Furthermore, this concentration was chosen for the current study for comparison of toxicological outcomes in C57BL/6 wild-type mice compared to those previously reported by our laboratory in atherosclerotic Apolipoprotein E null mice and human exposure models, as well as toxicological endpoints across organ systems [49,50,44]. For the exposures, mice were housed in an AAALC-approved facility, four to a cage, in standard shoebox cages within the 2 m^3 whole-body exposure chambers. The exposure rooms and chambers were maintained at 40–60 % relative humidity and a constant temperature (20–24 °C) throughout the exposures. Food was pulled daily during the exposures; however, mice had access to water *ad libitum*. All procedures involving animals were approved by the Institute's Animal Care and Use Committee (IACUC) at Lovelace Biomedical Research Institute / Lovelace Respiratory Research Institute and conform to the *Guide for the Care and Use of Laboratory Animals* published by the US National Institutes of Health (NIH Publication No. 85-23, revised 1996).

Mice from all exposure groups were anesthetized with Euthasol (at a dose of 0.1 mL per 30 g weight), and euthanized by exsanguination the morning following the last day of exposure (within 16 h) for tissue collection. The aorta, kidneys, and epididymal fat pad were carefully dissected, weighed, and split. One piece of each tissue was embedded in either TFM (VWR, Radnor, PA; the top half of left kidney and ascending aorta/arch) or 7.5 % gelatin (half of the adipose tissue pad) and frozen on dry ice; the remaining tissues were frozen in liquid nitrogen and stored at −80 °C (n = 8 per group).

2.2. Immunofluorescent staining of aorta and kidney tissues

Aorta and kidney tissues were fixed in Histochoice (VWR, 12 h at 4 °C), rehydrated in 30 % sucrose/1XPBS (12 h at 4 °C), embedded in TFM (Fisher Scientific), and sectioned on the cryostat at 7 μm. Sections were prepared for immunofluorescent detection of either AT1 receptor (1:1000 dilution; #ab18801, Abcam, Cambridge, MA), AT2 receptor (1:1000 dilution; #ab19134, Abcam), MOMA-2 (1:1000 dilution; #ab33451, Abcam), renin (1:500 dilution; # AF4277, R&D Systems), or TNF-α (1:1000 dilution; #ab1793, Abcam) and/or von Willebrand factor (vWF -aorta sections only – 1:1000 dilution; #ab11713, Abcam), using anti-sheep Alexa Fluor 488 or anti-goat Alexa Fluor 647 and secondary antibodies (double the concentration of primary antibody used; Thermo Fisher Scientific). All slides were imaged and analyzed using Image J software (NIH, Bethesda, MD), as previously described by our laboratory [45]. Total fluorescence was quantified per unit area in kidneys and aortas; colocalization (endothelial cells of the aorta) was determined by quantifying the overlaid signals' fluorescence from a minimum of 6 sections on 3 slides (n = 3–5 per group).

2.3. Dihydroethidium staining

Dihydroethidium staining of the aorta was processed and analyzed as previously described [51]. Briefly, dihydroethidium was prepared at a final concentration of 10 μmol/L in 1X PBS containing 20 % DMSO, applied to 7 μm thick aorta sections, cover-slipped, and incubated for 30 min in a dark, humidified chamber for 30 min. The resulting ethidium fluorescence was viewed using an emission at >580 nm and excitation of 510–550 nm, and fluorescence was quantified on the acquired digital images using Image J fluorescent densitometry (NIH), per unit area. A minimum of 4 tissue sections on 2 slides, n = 3 animals per study group was used to for analyses.

2.4. Tissue preparation and H& E morphology staining for adipose

Adipose tissue sections were fixed in a 1X zinc formalin fixative (Sigma Aldrich, St. Louis, MO) for 12 h, and then rehydrated in sucrose buffer (30 % in PBS, w/v) overnight. Tissue was then embedded in 7.5 % gelatin/1X PBS, solidified on a dry ice block, sectioned at 10 μm on a cryostat, placed on Poly-L Lysine slides (Thermo Fisher Scientific, Waltham, MA), and then processed through H&E, Nile Red, or immunofluorescent staining. Remaining tissue samples/slides were stored at -80 °C. For H&E staining of adipose, the slides were air-dried at RT for 15 min, fixed in ice-cold 1:1 methanol:acetone solution for 30 min, and rinsed 2x for 5 min each in 1X PBS. Slides were then stained with hematoxylin (1 min RT), rinsed in PBS, and then counterstained with eosin (30 s at RT), rinsed in PBS, cover-slipped, and imaged on an EVOS XL Core (Thermo Fisher Scientific) at 20x and 40x for analysis. A blinded participant measured the adipocytes. 40x images were used, and a minimum of 4–15 adipocytes were measured on each section, 8–10 sections from each animal, for a total of at least 100 cells per animal, and n = 4–5 animals per group, using Image J software (NIH). All adipocytes were measured along the longest axis in the view/plane for each measurement.

2.5. Nile Red and Perilipin staining of adipose tissue

10 μm thick adipose tissue sections were removed from the -80 °C, air-dried at RT for 30 min, fixed in ice-cold 1:1 methanol:acetone solution for 20 min, and rinsed 2x for 5 min each in 1X PBS. The tissues were then blocked for 60 min in 3% BSA/Tween and incubated with 150 μL (per section) perilipin antibody conjugated to AlexaFluor 488 (Invitrogen, Carlsbad, CA, #PA1−1051-A488, 1:1000 dilution) overnight at 4 °C. The tissue was rinsed 3x in 1x PBS. Slides were then stained with 150 μL (per section) of Nile Red solution (1:1000 of Nile Red solution into 0.3 % Triton X in 1X PBS) and incubated at RT in the dark for 10 min. Slides were rinsed for 5 min in 1X PBS, counterstained with 150 μL (per section) of 1:10,000 Hoechst nuclear stain in 1X PBS, and then rinsed 5 min at RT, and cover-slipped. Sections were imaged on the EVOS FL (Thermo Fisher Scientific) at 20x and 40x for analysis. A minimum of 8 sections per animal, 4–5 animals per group, were imaged and analyzed for total fluorescence and normalized by total cell count. Images were analyzed using ImageJ version 1.52p. Briefly, after using a subset of images to determine the optimal processing parameters, a macro was created and used on each image to acquire the necessary data (see Supplemental files for code). The macro accepted an RGB overlay image as input, which was then split into red, green, and blue channels. A threshold was then applied to each channel to ignore any background, and objects were traced using "Create Selection". Since the blue channel (nuclei) can often bleed over into the green channel at higher intensities, a mask was created to remove those areas on both red and green channels. The mean gray value for each sample was then normalized to the median nuclei count across all sections analyzed (to normalize expression per # of cells, since FA + HF and MVE + HF animals had much larger adipocytes and thus fewer cells per 40x image).

2.6. Immunofluorescent staining of adipose tissue

Slides were prepared as described for Nile Red staining. 150 μl of the appropriate primary antibody: AGT (R&D Systems, Minneapolis, MN, #AF6996; 1:500), AT1 receptor (Abcam, Cambridge, MA; #ab18801, 1:1000), AT2 receptor (Abcam #ab19134; 1:1000), TNF-α (Abcam #ab1793; 1:1000), MCP-1 (Novus Biologicals, Centennial, CO; #NBP2−22115, 1:1000), GLUT4 (Novus Biologicals, NBP1−49533; 1:250), or IR-β (#NBP2−12793; 1:500) was applied for immunofluorescence (or double immunofluorescence) for 1 h at RT, followed by another incubation for 1 h at RT with the appropriate secondary antibody conjugated to either Alexa Fluor 455 or Alexa Fluor 555 (Thermo Fisher Scientific; double the concentration of primary antibody used), imaged (10x, 20x, 40x), and analyzed, as previously published [52]. Total fluorescence was quantified per unit area and normalized to total either total area or adipocyte cell count from a minimum of 2 slides, 4 sections, n = 3–5 per group.

2.7. Real-time RT-qPCR

Adipose, vascular, or renal tissue gene expression of either AT1, AT2, TNF-α, MCP-1, angiotensinogen, or renin was quantified via real-time RT-qPCR, using the appropriate primers, listed in Supplementary Table 1. Briefly, a Qiagen AllPrep DNA/RNA/miRNA Universal Kit (Catalog #80224, Germantown, MD) was used to isolate RNA from kidney, vascular (aorta), and adipose tissue. A BIORAD CFX96 (Hercules, CA) was used for RT-qPCR reactions and analyses [50,44]. $\Delta\Delta C_T$ results were analyzed (GAPDH controls) in the aorta, kidney, or adipose tissues from an n = 7–8 animals from each study group.

2.8. Statistics

Graphed data represent either mean ± SD or mean ± SEM, as indicated in the figure legends. A two-way ANOVA with a post-hoc Tukey pair-wise multiple comparison analysis was used to determine the statistical relationships mediated by the exposure, diet, and/or exposure-diet interactions amongst all diet and exposure groups. Sigma Plot 12.0 software (Systat, San Jose, CA) was used to conduct statistical analyses. Statistical comparison values were considered statistically significant at $p \leq 0.05$.

3. Results

3.1. MVE-exposure with HF diet increases vascular AT1 receptor expression

Our laboratory has recently reported increased circulating Ang II in C57BL/6 wild-type mice exposed to MVE, which is further exacerbated in mice fed a HF diet. [44]. As increased Ang II – AT1 signaling is positively correlated to CVD progression, we analyzed vascular AT1 receptor expression in our study animals. Vascular (aortic) AT1 receptor expression was observed to be significantly elevated in the FA + HF, MVE + LF, and MVE + HF groups (Fig. 1 panels and Fig. 1A, $p < 0.001$). The respective F-values for exposure = 44.25, diet = 19.29, with no exposure-diet interaction observed. Vascular AT1 receptor expression was increased in the MVE + HF animals compared to both the MVE + LF and FA + HF animals, as determined through pairwise comparison (Fig. 1A). While we quantified the total vascular expression of the AT1 receptor in the aorta sections, the highest expression was observed in the vascular endothelial cell layer. Similar trends in expression were quantified in vascular AT1 receptor at the mRNA transcript level in MVE-exposed animals, compared to FA control animals (Fig. 1B, $p < 0.001$ and $p = 0.039$ for MVE + LF); however, AT1 mRNA was not statistically significant in the FA + HF group, when compared to the FA + LF group (Fig. 1B, $p = 0.117$).

3.2. MVE-exposure promotes the expression of vascular factors associated with CVD

As sequestration and infiltration of monocytes/macrophages into the vessel wall is a hallmark of atherosclerosis, we analyzed vascular monocyte/macrophage infiltration in our study animals using MOMA-2 staining. Our results showed that compared to the aortas of FA animals (Fig. 2A), MVE-exposure mediated a significant induction of vascular MOMA-2 staining, regardless of diet consumed (Fig. 2A), quantified in Fig. 2B. The F-value for exposure = 20.457, $p < 0.001$. No statistical difference was observed between the FA + LF vs. FA + HF group and no exposure-diet interaction for vascular MOMA-2 staining.

Increased levels of VCAM-1 and ICAM-1 in both tissue and circulation are early biomarkers for the pathogenesis of atherosclerosis [5,6]; thus, we analyzed their transcript expression in the aortas from our animals on study. Vascular ICAM-1 mRNA was significantly elevated in the MVE + LF group, compared to FA controls (Fig. 2C, $p = 0.039$). The MVE + HF group showed a more significant induction of ICAM-1 mRNA compared to both the MVE + LF and FA controls (Fig. 2C, $p < 0.001$ for each comparison); there was a statistically significant interaction between exposure and diet for vascular ICAM-1 expression ($p = 0.039$; $F = 4.69$). There was no difference between ICAM-1 transcript expression in the LF + FA vs. HF + FA group ($p = 0.141$). Vascular VCAM-1 mRNA expression (Fig. 2D) was also increased in the MVE + HF group, compared to the MVE + LF ($p = 0.011$), FA + HF ($p = 0.007$), and the FA + LF ($p = 0.005$) groups, but no differences in expression between any of the other groups, nor an exposure-diet interaction for expression of vascular VCAM-1.

Since elevated ROS production is associated with the pathogenesis of CVD, we analyzed vascular ROS using dihydroethidium (DHE) staining. Compared to the FA + LF group, there was a significant increase in DHE staining in the vasculature of the FA + HF group (Fig. 3A, $p < 0.001$). Furthermore, DHE staining was also elevated in the MVE + LF animals (Fig. 3A and B, $p = 0.027$), compared to FA + LF controls, with a more significant induction observed in the vasculature of the MVE + HF group (Fig. 3B, $p < 0.001$ compared to MVE + LF group). The respective F-values were exposure = 4.87, diet = 79.09; there was no significant interaction between exposure and diet.

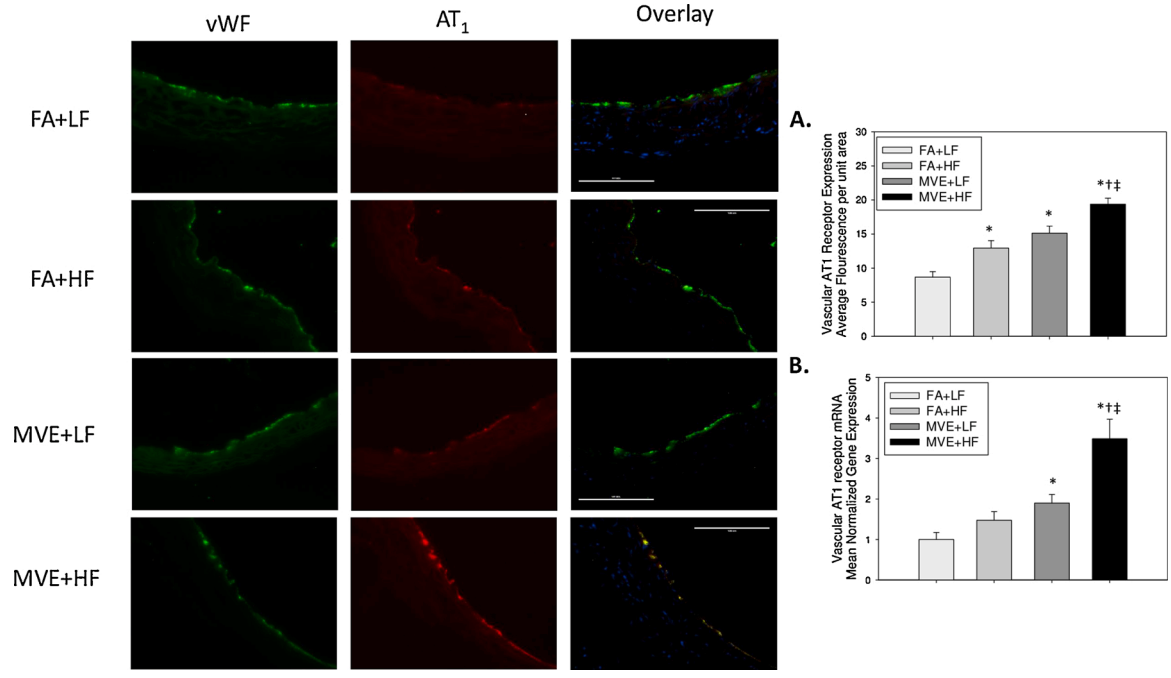

Fig. 1. Representative images of vascular Angiotensin II type 1 receptor (AT1, red) and von Willebrand endothelial marker (vWF, green) expression in the aorta of male C57BL/6 mice exposed via inhalation to either filtered air (FA) while fed a low-fat (LF) diet, FA while fed a high-fat (HF) diet, 100 μg PM/m^3 of mixed vehicle emissions (MVE) while fed a LF diet or MVE while fed a HF diet. All MVE and FA control exposures were conducted for 6 h/d, 7 d/wk, for a period of 30 d. Overlay = yellow fluorescence. Blue = Hoechst nuclear stain. (A) Fluorescence quantification of vascular AT1 receptor expression (4 sections each; n = 4 per exposure group). Fluorescence of endothelial cell-specific AT1 receptor expression was quantified from the overlay image f0b1; SEM. 40x magnification; scale bar = 100 μm. (B) Vascular AT1 receptor mRNA quantification by real-time qPCR (n = 8). *$p \leq 0.05$ compared to FA + LF; †$p \leq 0.05$ compared to FA + HF; ‡$p \leq 0.05$ compared to MVE + LF using a 2-way ANOVA.

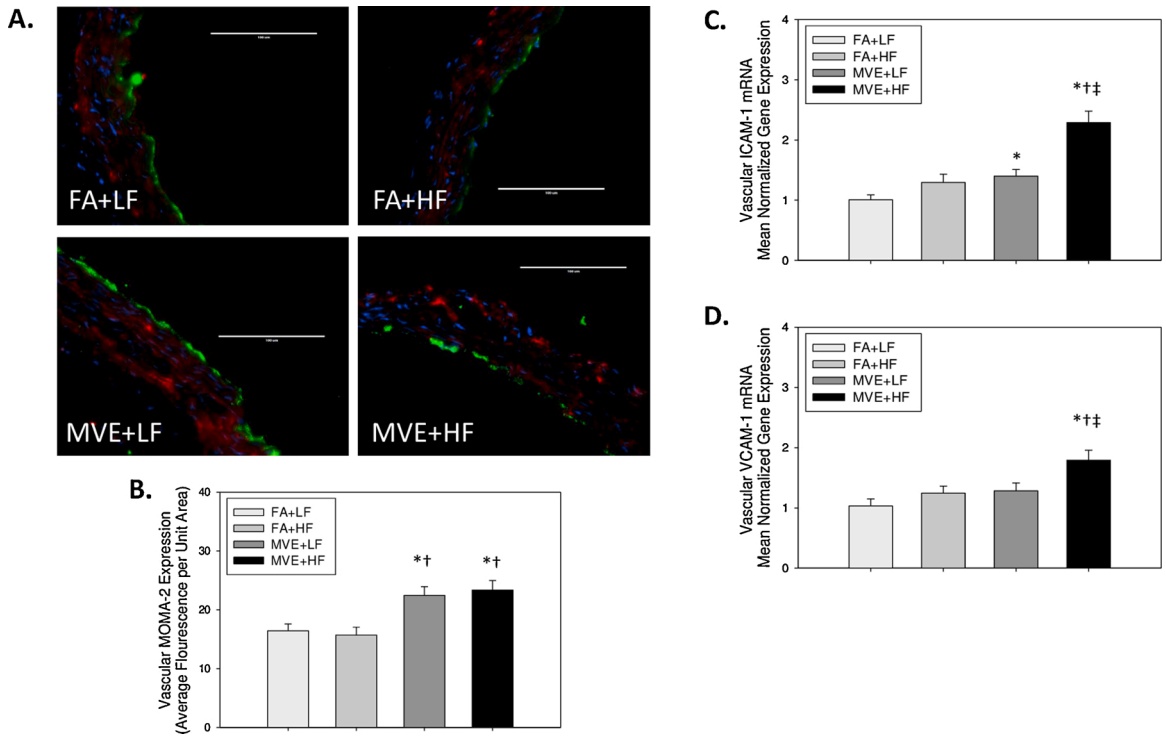

Fig. 2. Representative images of (A) monocyte/macrophage marker MOMA-2 (red) in the aorta of male C57BL/6 mice exposed via inhalation to either filtered air (FA) while fed a low-fat (LF) diet, FA while fed a high-fat (HF) diet, 100 μg PM/m^3 of mixed vehicle emissions (MVE) while fed a LF diet or MVE while fed a HF diet. All MVE and FA control exposures were conducted for 6 h/d, 7 d/wk, for a period of 30 d. Green fluorescence = vWF; blue = Hoechst nuclear stain. 40x magnification; scale bar = 100 μm. (B) Fluorescence was measured, graphed, and data are shown as mean per unit area f0b1; SEM (4 sections each; n = 4 per exposure group). Real-time RT-qPCR analysis of vascular mRNA expression of (C) intracellular adhesion molecule (ICAM) -1, and (D) vascular cell adhesion molecule (VCAM)-1 in aortas from C57BL/6 mice from each study exposure/diet group (n = 8 per group). Data are expressed as mean normalized gene expression using ΔΔCT values, with GAPDH used as the house-keeping gene. *p ≤ 0.05 compared to FA + LF; †p ≤ 0.05 compared to FA + HF; ‡p ≤ 0.05 compared to MVE + LF using a 2-way ANOVA.

3.3. Inhalation MVE-exposure results in increased kidney renin expression

To analyze the effects of MVE exposure on other components of the systemic RAS signaling pathway, we quantified the kidney expression of renin at both the protein and transcript levels. At the protein level, compared to FA controls, the immunofluorescent analysis showed increased kidney renin expression in animals exposed to MVE (Fig. 4A and B, $p < 0.001$). There was no observed change in kidney renin expression between the FA + LF and FA + HF groups. The F-value for exposure = 58.81; there was no statistical contribution of diet or exposure-diet interaction for kidney renin expression, as summarized in Fig. 4B. In agreement with these findings, MVE-exposure was also associated with increased kidney renin mRNA expression (Fig. 4C, $p = 0.025$; $F = 5.68$), but not with diet ($p = 0.161$; $F = 2.08$), compared to the respective FA controls (Fig. 4C). While kidney renin levels were altered with MVE-exposure, kidney AGT mRNA expression was not statistically different across any exposure or diet groups (Supplemental Fig. 1A)

3.4. Kidney angiotensin receptor expression is altered with exposure to MVE

To determine the effects of MVE exposure on renal Ang II receptor expression, we analyzed both AT1 and AT2 in the kidneys. Compared to FA controls, MVE- exposed animals displayed elevated AT1 receptor expression in the kidney, regardless of diet (Fig. 5A and B, $p < 0.001$; $F = 24.16$), with no significant diet-exposure interaction noted, as summarized in Fig. 2B. When quantifying renal AT1 mRNA transcript levels, only the HF + MVE group was statistically elevated compared to FA + LF controls (Fig. 5C, $p = 0.029$; $F = 5.29$).

Similarly, for renal AT2 receptor expression, compared to FA controls, we also noted that MVE-exposure results in increased kidney AT2 receptor expression (Fig. 5D and E, $p < 0.001$; $F = 24.06$), which appears to be further increased with the consumption of a HF diet (Fig. 5E; MVE + LF vs. MVE + HF, $p = 0.014$). There was no observed change in renal AT2 expression in the FA + LF vs. FA + HF groups, nor was there a significant interaction between exposure and diet. Interestingly, there were no statistical differences noted across any of the diet or exposure groups for expression of renal AT2 mRNA (Fig. 5F).

3.5. Inhaled MVE-exposure mediates increased adipose weight and adipocyte size

As abnormal RAS signaling is associated with adipose tissue growth and obesity [53], we quantified body weight changes, epididymal fat pad weight, and adipocyte size. Animals were randomly grouped and placed on their respective diets 30d before the onset of exposures (day 0). As expected, at the beginning of the exposures (day 30), the HF diet animals weighed significantly more than the LF diet animals (Fig. 6A). At the end of the exposure study (day 60), the HF diet animals still had significantly increased body weights compared to the LF diet animals; however, the MVE + HF body weights were also statistically elevated compared to the FA + HF body weights (Fig. 6A, $p = 0.005$). A two-way ANOVA showed that both exposure ($p = 0.010$, $F = 7.70$) and diet ($p < 0.001$, $F = 51.90$) mediated alterations in body weight; no statistical interaction between exposure and diet was noted. In agreement with these findings, compared to the FA + LF animals, we observed a significant increase in the epididymal fat pad weight in the FA + HF, MVE + LF, and MVE + HF groups (Fig. 6B). The two-way ANOVA

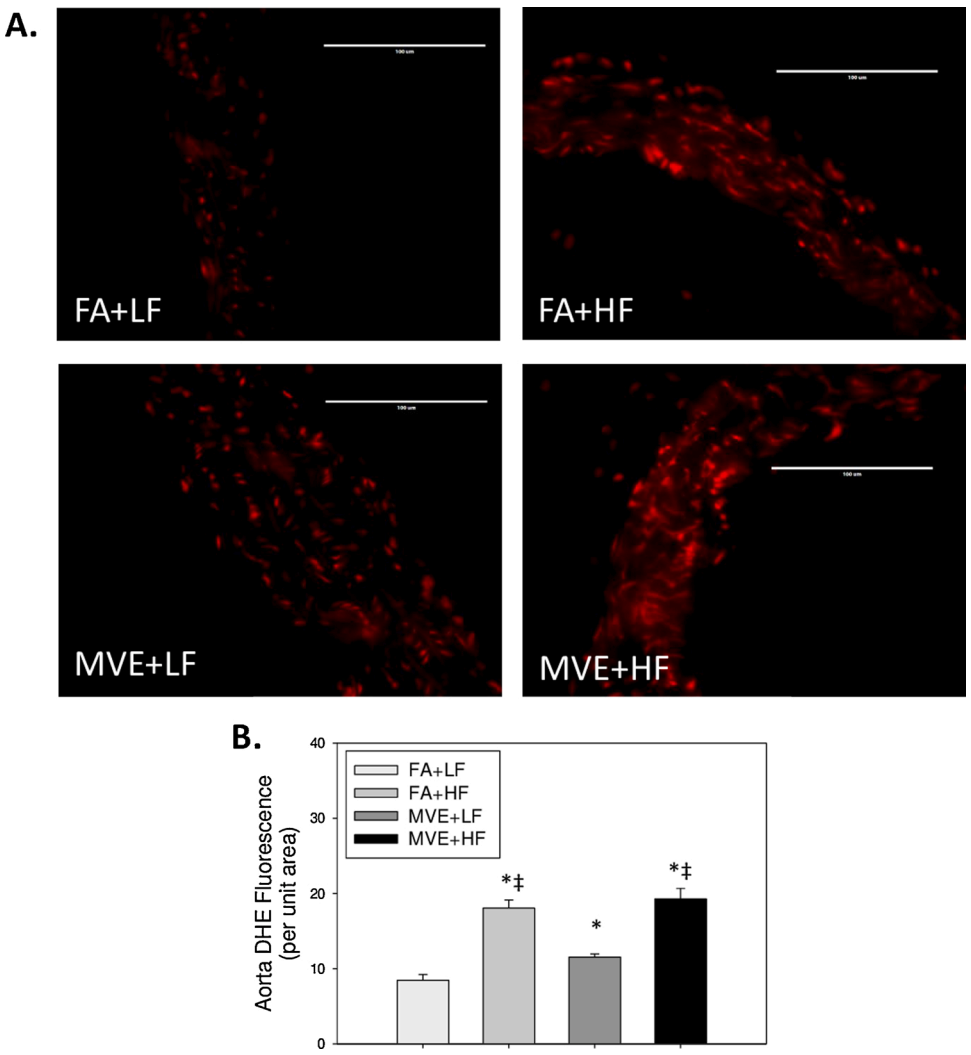

Fig. 3. Representative images of dihydroethidium (DHE) staining (red) in the aorta of male C57BL/6 mice exposed via inhalation to either filtered air (FA) while fed a low-fat (LF) diet, FA while fed a high-fat (HF) diet, 100 μg PM/m^3 of mixed vehicle emissions (MVE) while fed a LF diet or MVE while fed a HF diet. All MVE and FA control exposures were conducted for 6 h/d, 7 d/wk, for a period of 30 d. (B) Fluorescence was measured, graphed, and is shown as mean f0b1; SEM (4 sections each; n = 3 per exposure group). 40x magnification; scale bar = 100 μm. *p ≤ 0.05 compared to FA + LF; ‡p ≤ 0.05 compared to MVE + LF using a 2-way ANOVA.

analysis showed that both exposure ($p < 0.001$; $F = 19.35$) and diet ($p < 0.001$, $F = 70.28$) significantly contributed to epididymal fat pad weights (Fig. 6B). Furthermore, the epididymal fat pad weight in the MVE + HF group was significantly higher when compared to the MVE + LF ($p < 0.001$) and FA + HF (Fig. 6B, $p = 0.004$) groups. There was no significant exposure-diet interaction observed in epididymal fat pad weights. When adjusted for body weight, using the formula [(epididymal fat pad weight) / (bodyweight)] x 100, there is a significant increase in adiposity in the HF diet groups compared to the LF diet groups, which is further exacerbated in the MVE + HF group (Fig. 6C; $p = 0.002$ compared to FA + HF). Adiposity in the MVE + LF group was not significant compared to the FA + LF group (Fig. 6C, $p = 0.059$).

When measuring adipocyte size in the epididymal fat pad, compared to FA + LF controls, we observed adipocyte hypertrophy in the FA + HF (Fig. 7A, $p < 0.001$), MVE + LF (Fig. 7A, $p < 0.001$), and MVE + HF (Fig. 7A, $p < 0.001$) groups, as determined through the post-hoc all-pairwise multiple comparison analysis. Adipocyte size in the MVE + HF group was also significantly increased compared to both the MVE + LF ($p < 0.001$) and FA + HF ($p < 0.001$) groups (Fig. 7A). A two-way ANOVA of adipocyte average size across study groups (Fig. 7B) showed that the increase in adipocyte size was mediated by diet ($p < 0.001$, $F = 200.22$) and exposure ($p < 0.001$, $F = 100.49$), with a statistically significant interaction between exposure and diet ($p < 0.001$, $F = 23.32$).

3.6. Increased lipid accumulation with HF diet, but not MVE-exposure

To determine if the exposure mediated increases in adipocyte size were associated with increased lipid accumulation, a Nile Red analysis was performed. (Fig. 8; red fluorescence). Additionally, we analyzed perilipin, a phosphoprotein on the surface of adipose lipid droplets that regulates lipolysis (Fig. 8; green fluorescence) often found upregulated in obesity [54]. Compared to FA + LF and MVE + LF animals, we observed a significant increase in Nile Red fluorescence, indicative of lipid accumulation, in both the FA + HF and MVE + HF adipose tissue (Fig. 8; red fluorescent panels). Even when normalized to the cell count per unit area (since the MVE + HF group had fewer cells per unit area due to adipocyte hypertrophy), there was such intragroup variability that there was no statistical difference between the FA + HF and MVE + HF groups (Fig. 8A, $p = 0.124$). The two-way ANOVA analysis showed that lipid accumulation was mediated by diet ($F = 8.381$, $p = 0.020$), but not exposure ($F = 1.707$, $p = 0.228$), and there was no diet-exposure interaction observed. We did not observe any difference in perilipin expression across any of the groups, as shown in Fig. 8B.

3.7. Adipocyte RAS pathway is increased with MVE-exposure and HF diet

To determine whether MVE-exposure alters the local adipocyte RAS system, we analyzed adipocyte expression of AGT, and the AT1 and AT2 receptors, at both the protein and mRNA transcript level. Compared to FA + LF controls, AGT expression was elevated in FA + HF, though not

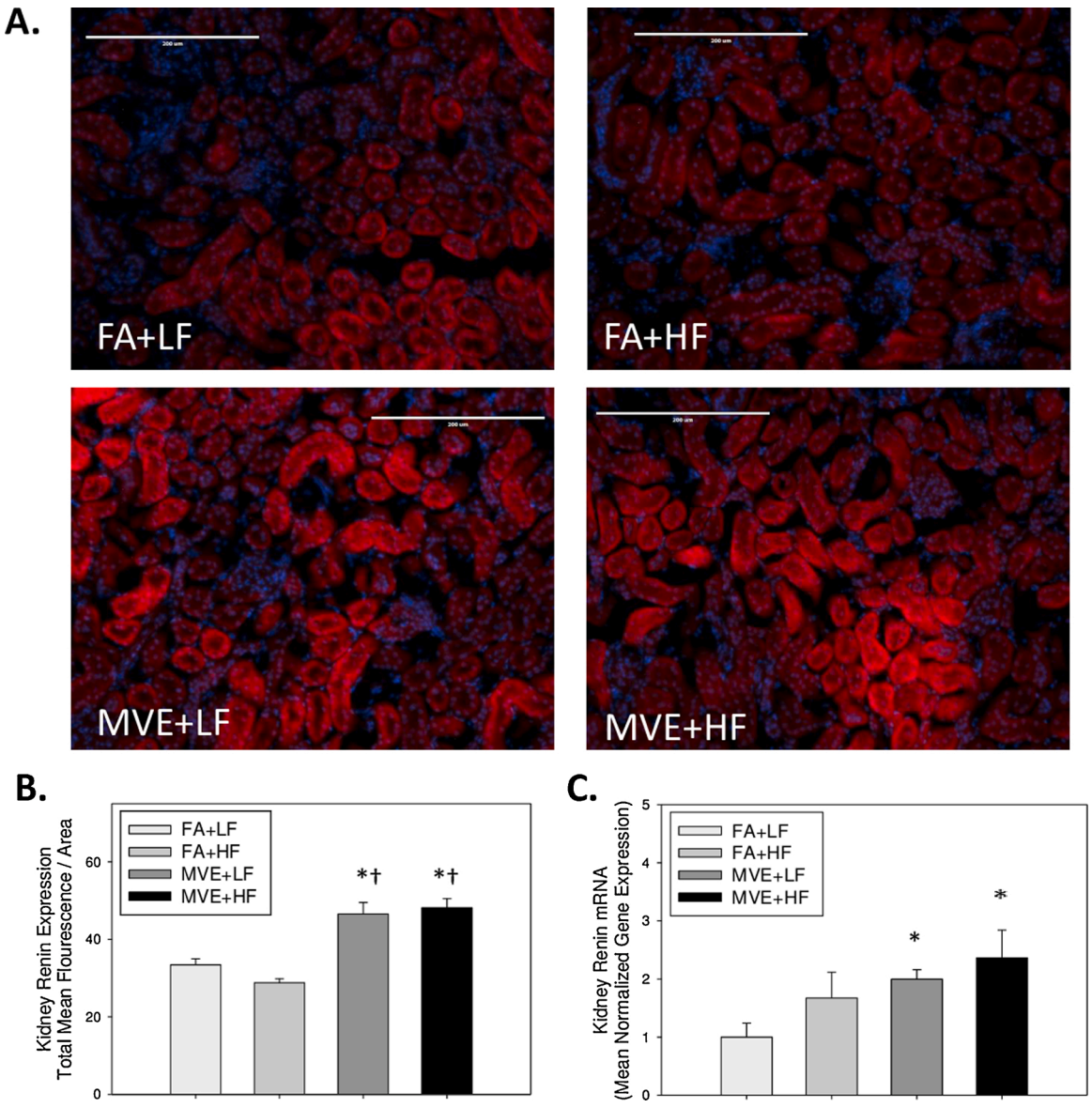

Fig. 4. Representative images of renin expression (red) in the kidney of male C57BL/6 mice exposed via inhalation to either filtered air (FA) while fed a low-fat (LF) diet, FA while fed a high-fat (HF) diet, 100 μg PM/m^3 of mixed vehicle emissions (MVE) while fed a LF diet or MVE while fed a HF diet. All MVE and FA control exposures were conducted for 6 h/d, 7 d/wk, for a period of 30 d. Blue = Hoechst stained nuclei. (B) Fluorescence was measured, graphed, and is shown as mean f0b1; SEM (4 sections each; n = 3-5 per exposure group). 20x magnification; scale bar =200 μm. (C) Kidney renin mRNA expression, as determined by real-time RT-qPCR (n = 7-8 per group). *$p \leq 0.05$ compared to FA + LF; †$p \leq 0.05$ compared to FA + HF using a 2-way ANOVA.

statistically (Fig. 9A, $p = 0.52$). AGT expression was significantly increased in both MVE + LF and MVE + HF exposure groups, compared to the FA control groups (Fig. 9A and B, $p < 0.001$, $F = 54.92$), with a statistical increase in AGT in the MVE + HF group when compared to the MVE + LF group (Fig. 9A and B, $p = 0.009$). Real-time RT-qPCR data showed that the MVE + HF group has a significant elevation in adipose AGT mRNA expression (Fig. 9C), compared to all other study groups, with a significant interaction between exposure and diet ($p = 0.002$; $F = 12.113$).

When analyzing AT1 and AT2 receptor expression in adipose tissue from the epididymal fat pad, compared to FA controls, expression of the AT1 receptor was increased in the adipose tissue of MVE-exposed mice (Fig. 10A, $p = 0.003$, $F = 10.46$ for exposure). In the MVE + HF group, the expression of the AT1 receptor was further increased, compared to the MVE + LF group (Fig. 10A, $p = 0.001$). There was also a statistical difference noted in adipose AT1 expression in the FA + LF compared to the FA + HF groups (Fig. 10A, $p = 0.004$; $F = 22.46$ for diet). There were no significant interactions measured between exposure and diet ($p = 0.912$; $F = 0.012$). Conversely, no difference was observed between adipose AT2 expressions across any groups (Fig. 10B). At the mRNA transcript level, only the MVE + HF group showed an increase in adipose AT1 receptor mRNA expression (Fig. 11A), compared to both the FA groups ($p = 0.002$; $F = 12.26$) and the MVE + LF group ($p = 0.003$). When analyzing transcript levels of AT2 receptors in the adipose tissue (Fig. 11B), no significant differences were observed between any of the groups.

3.8. MVE-exposure alters adipokine and adipose inflammatory marker expression

Since altered RAS signaling is associated with a "pro-inflammatory" signaling phenotype in adipose tissue, we next investigated whether MVE exposure ± HF diet alters the expression of adipokines (leptin and adiponectin) or inflammatory markers (TNF-α, IL-6, and MCP-1) in the

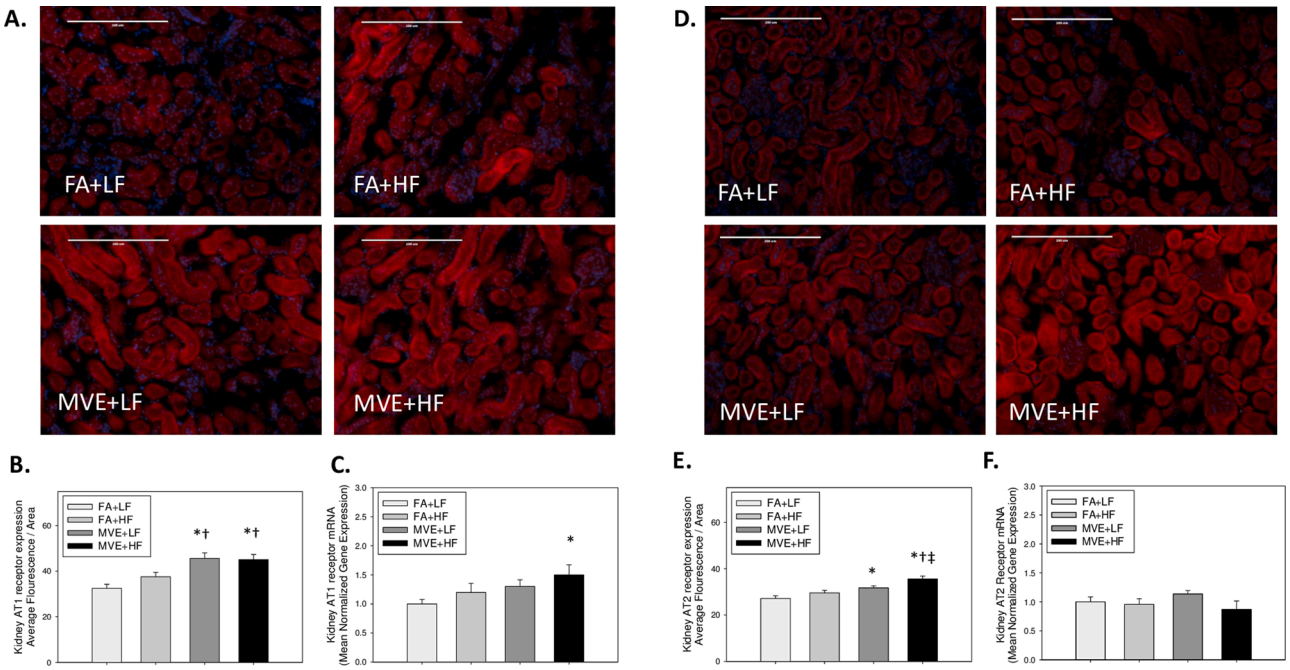

Fig. 5. Representative images of (A) AT1 receptor expression (red) in the kidney of male C57BL/6 mice exposed via inhalation to either filtered air (FA) while fed a low-fat (LF) diet, FA while fed a high-fat (HF) diet, 100 μg PM/m^3 of mixed vehicle emissions (MVE) while fed a LF diet or MVE while fed a HF diet. All MVE and FA control exposures were conducted for 6 h/d, 7 d/wk, for a period of 30 d. Blue = Hoechst stained nuclei. (B) AT1 fluorescence was measured, graphed, and is shown as mean f0b1; SEM (4 sections each; n = 5 per exposure group). Blue = Hoechst nuclear stain. 20x magnification; scale bar =200 μm. (C) Kidney AT1 mRNA expression, as determined by real time RT-qPCR (n = 7-8 per group). (D) Representative images of AT2 expression (red) in the kidney of male C57BL/6 mice. (E) AT2 fluorescence was measured, graphed, and is shown as mean f0b1; SEM (4 sections each; n = 5 per exposure group). 20x magnification; scale bar =200 μm. (F) Kidney AT2 mRNA expression, as determined by real time RT-qPCR (n = 7-8 per group). *p ≤ 0.05 compared to FA + LF; †p ≤ 0.05 compared to FA + HF; ‡p ≤ 0.05 compared to MVE + LF using a 2-way ANOVA.

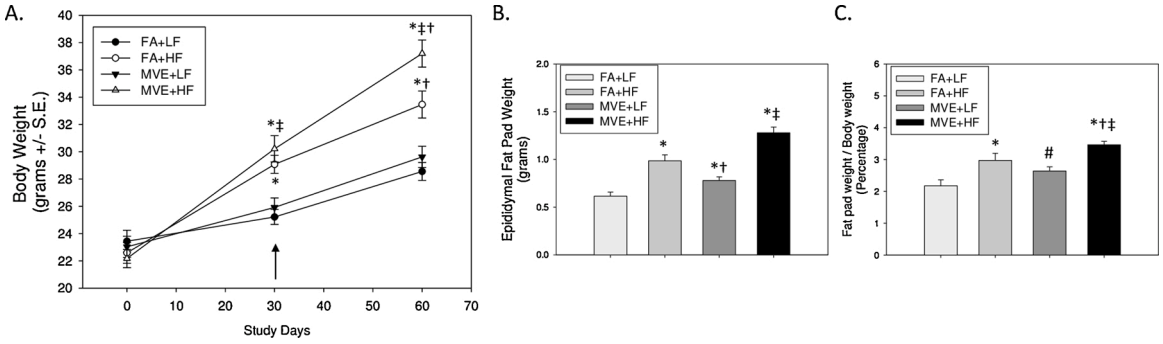

Fig. 6. Animal study weights for (A) body weight, (B) epididymal fat pad weight (wet weight), and (C) fat pad/body weight (BW) ratio for male C57BL/6 mice exposed via inhalation to either filtered air (FA) while fed a low-fat (LF) diet, FA while fed a high-fat (HF) diet, 100 μg PM/m^3 of mixed vehicle emissions (MVE) while fed a LF diet or MVE while fed a HF diet. All MVE and FA control exposures were conducted for 6 h/d, 7 d/wk, for a period of 30 d. Animals were placed on a HF diet 30d prior to the initiation of the study. The inhalation exposures began on study day 30, which is indicated by the arrow in the graph in panel (A). Values shown are ± S.E. *p ≤ 0.05 compared to FA + LF; †p ≤ 0.05 compared to FA + HF; ‡p ≤ 0.05 compared to MVE + LF; and #p = 0.059 compared to FA + LF using a 2-way ANOVA.

adipose tissue. In the MVE + HF group, the two-way ANOVA showed a significant increase in adipose leptin mRNA expression compared to all other groups (Fig. 11C). We also observe an alteration in adiponectin expression in the adipose tissue with HF diet and MVE-exposure (Fig. 11D); however, because of the vast intragroup variability, there were no statistically significant relationships measured.

When analyzing the expression of inflammatory markers in the adipose tissue, MVE-exposure mediated an increase in IL-6 transcript expression, regardless of diet (Fig. 11E, $p < 0.001$; $F = 40.21$). Moreover, both diet ($p < 0.001$, $F = 19.36$) and the interaction between exposure and diet ($p = 0.012$, $F = 7.16$) showed a significant interaction for adipose IL-6 transcript expression. Interestingly, there was no alteration in adipose TNF-α expression at either the protein (Supplemental Fig. 2A and B) or transcript level (Supplemental Fig. 2C) across any diet or exposure group. Conversely, compared to FA animals, there was a statistical increase in MCP-1 in the adipose tissue of animals exposed to MVE on both diets, at both the protein (Fig. 12A and B: MVE + LF, $p = 0.030$; MVE + HF, $p < 0.001$) and mRNA transcript level (Fig. 12C). Similar to adipose IL-6 expression, there is a statistically significant interaction between exposure and diet at the protein ($p < 0.001$, $F = 17.10$) and transcript ($p = 0.002$; $F = 12.11$) levels of adipose MCP-1.

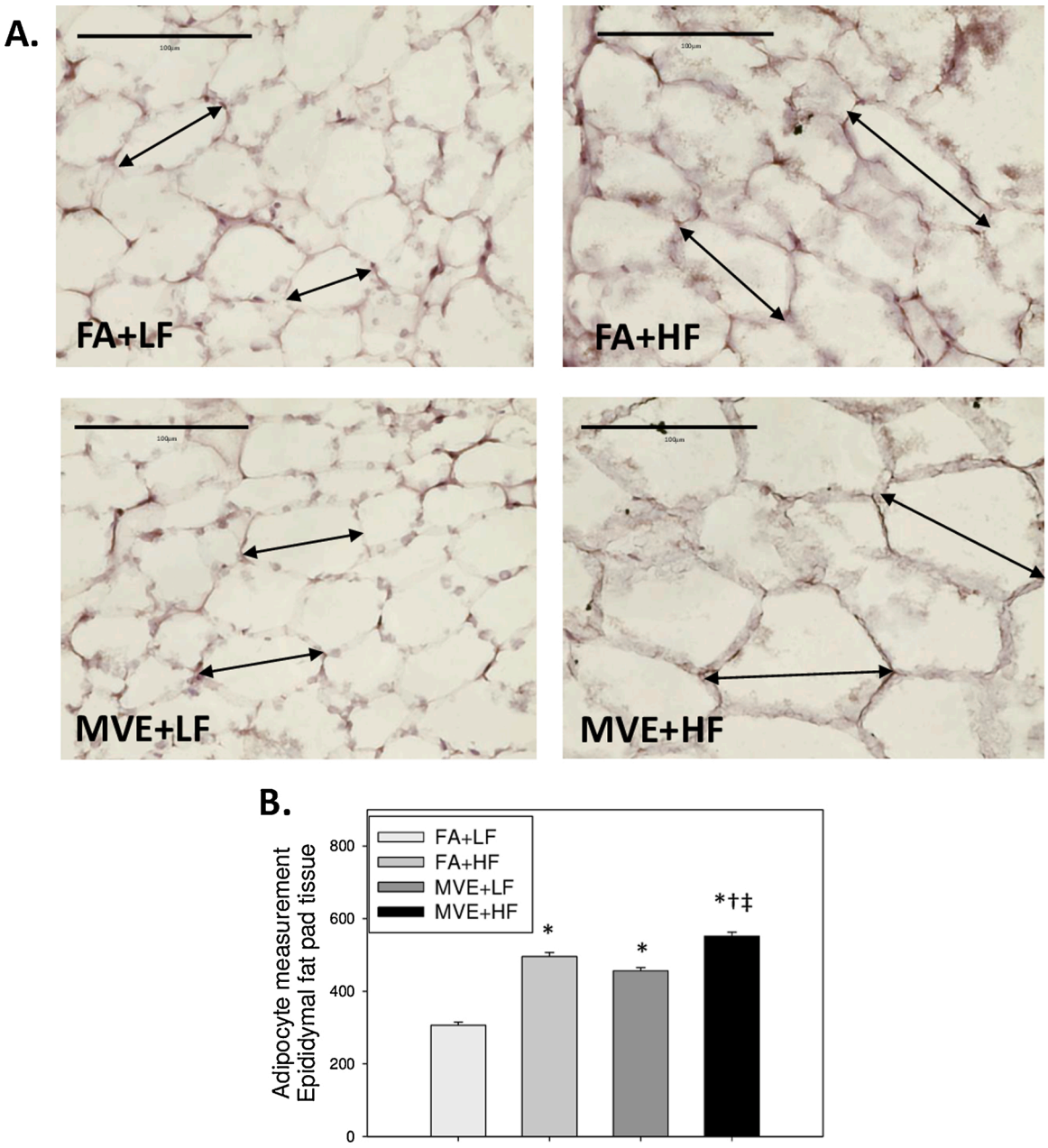

Fig. 7. Representative images of H&E staining of adipocytes from the epididymal fat pad of male C57BL/6 mice exposed via inhalation to either filtered air (FA) while fed a low-fat (LF) diet, FA while fed a high-fat (HF) diet, 100 μg PM/m^3 of mixed vehicle emissions (MVE) while fed a LF diet or MVE while fed a HF diet. All MVE and FA control exposures were conducted for 6 h/d, 7 d/wk, for a period of 30 d. n = 4-5 per exposure group, 8 sections each, a minimum of 100 adipocytes measured. (B) Measurements across the longest side of the adipocyte were quantified and represented as mean f0b1; S.E. 40x magnification; scale bar = 100 μm. *p ≤ 0.05 compared to FA + LF; †p ≤ 0.05 compared to FA + HF; ‡p ≤ 0.05 compared to MVE + LF using a 2-way ANOVA.

3.9. MVE-exposure reduces adipose GLUT4 and insulin receptor expression

Since alteration in glucose uptake is associated with increased fat storage in adipocytes ([55]; [56]), we also analyzed the expression of the GLUT4 receptor in the adipose tissue. We observed differential effects of MVE-exposure on GLUT4 expression in adipose tissue, dependent on diet. Compared to the FA + LF, we observed a decrease in GLUT4 in the adipose of the FA + HF group (Fig. 13A and B, p = 0.004). There was no statistical change in adipose GLUT4 levels in the MVE + LF group; however, there was a significant decrease in GLUT4 expression in adipose tissue from the MVE + HF group, compared to all other groups (Fig. 13A), as quantified in Fig. 13B. Pairwise comparison showed a statistical difference in adipose GLUT4 expression in the MVE + HF group compared to both the MVE + LF (p < 0.001) and FA + HF (p = 0.012) groups. The two-way ANOVA analysis showed a significant interaction between exposure and diet in mediating GLUT4 expression in the adipose tissue from these study animals (p = 0.007, F = 7.72).

Insulin is responsible for regulating glucose uptake via GLUT4 stimulation and has been reported to mediate adipocyte growth and differentiation [57]. Thus, we quantified insulin receptor-beta (IR-β) expression in the adipose tissue of our study animals. We measured a significant increase in IR expression in MVE + LF adipose tissue, compared to FA + LF mice (Fig. 13C, p = 0.007), but not in the FA + HF. Conversely, compared to animals from all other study groups, there was a decrease in IR-β expression in the adipose tissue from the MVE + HF study animals (Fig. 13D). The two-way ANOVA analysis

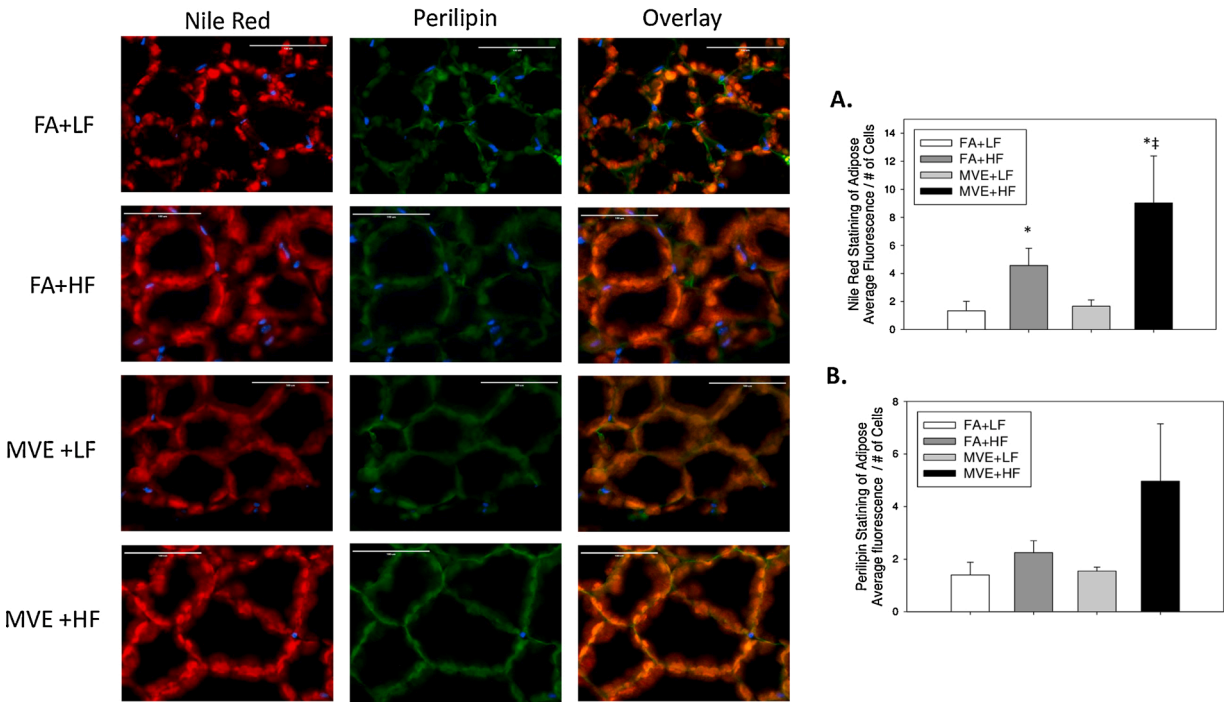

Fig. 8. Representative images of epididymal adipose tissue lipid staining (Nile Red, red) and perilipin immunofluorescence (perilipin, green) expression in male C57BL/6 mice exposed via inhalation to either filtered air (FA) while fed a low-fat (LF) diet, FA while fed a high-fat (HF) diet, 100 μg PM/m^3 of mixed vehicle emissions (MVE) while fed a LF diet or MVE while fed a HF diet. All MVE and FA control exposures were conducted for 6 h/d, 7 d/wk, for a period of 30 d. Overlay = yellow fluorescence. Blue = Hoechst nuclear stain. (A) Nile Red and (B) perilipin fluorescence was measured and shown as mean fluorescence / # cells ± SEM (6-8 sections each; n = 3-4 per exposure group), using the 40x magnification images. Scale bar = 100 μm. *p ≤ 0.05 compared to FA + LF; ‡p ≤ 0.05 compared to MVE + LF using a 2-way ANOVA.

reported a significant interaction between exposure and diet ($p < 0.001$, $F = 20.45$).

4. Discussion

CVD is one of the most significant public health problems globally, accounting for more deaths than any other cause worldwide [4]. In the United States alone, CVD affects approximately 92.1 million people over 20 years of age [58]. Air pollution exposure and obesity are known to be independent risk factors for CVD, including atherosclerosis [59]; rev. in [2,3]. Obese individuals may be at higher risk for air pollution-induced CVD progression, as they take in more air per day than those of a healthy weight [60]. Obesity is growing in prevalence, with worldwide obesity rates in children and adults tripling since 1975 [61]. Air pollution exposure, including traffic-generated pollutants, has recently emerged as a likely contributor to metabolic dysfunction and obesity in both adults and school-aged children (rev. in [62,63,15,16,64]). As it is estimated that within urban areas, greater than 80 % of the population are exposed to air pollution levels that exceed WHO limits [1]; therefore, it is imperative to understand the mechanisms by which air pollution exposure mediates CVD and obesity comorbidities.

Both CVD and obesity have multifactorial etiologies, including genetics, diet, hormones, activity levels, and environmental exposures. Dysregulation of RAS signaling is associated with the pathophysiology of CVD and obesity (rev. in [65]; rev in. [66]). Thus, we investigated whether MVE exposure ± HF diet altered systemic or adipose (local) RAS signaling. In the current study, we observed a significant elevation in the renal expression of renin expression in MVE-exposed mice. These results agree with our previously reported findings of increased circulating Ang II in the MVE + LF and MVE + HF mice, compared to both FA control groups [44]. The conversion of AGT ⟶ Ang I, by renin, is believed to be the rate-limiting step for Ang II generation in most physiological pathways. Therefore, increased renin production in kidneys of MVE-exposed mice is likely correlated to the elevated plasma Ang II levels also observed in these mice. We also observed an increase in renal AT1 (protein and mRNA) and AT2 receptors (protein only) in MVE-exposed animals, regardless of the diet. In the kidney, signaling through the AT1 vs. AT2 receptor has opposing physiologic effects. For example, Ang II - AT1 signaling in the kidney regulates vasoconstriction, sodium/water reabsorption, and promotes fibrosis and cellular growth and proliferation. Conversely, Ang II-AT2 signaling increases the production of vasodilators, bradykinin, and nitric oxide and promotes cell differentiation and apoptosis in the kidney (rev. in [67]). As increased renal AT1 signaling is known to be associated with renal injury, it is plausible that the observed elevation in AT2 receptors is a compensatory mechanism to protect the kidneys in the MVE-exposed animals. We did not observe any alterations in renal AGT expression (Supplemental Fig. 1A) or inflammatory marker TNF-α (Supplemental Fig. 1B) mRNA expression across any groups. Interestingly, chemokine MCP-1 mRNA was downregulated in the kidneys of C57BL/6 mice exposed to MVE, regardless of diet, compared to FA controls (Supplemental Fig. 1C). MCP-1 deficient mice show increased apoptosis and renal damage after ischemia/reperfusion injury, suggesting that MCP-1 protects the kidney during acute inflammatory responses [68]. Thus, MVE-exposure may contribute to kidney injury via diminished MCP-1 expression, though we did not directly analyze this in the present study.

In conjunction with increased plasma Ang II and kidney renin levels, we also observed increased vascular AT1 receptor expression in MVE + LF and MVE + HF C57BL/6 mice. This finding agrees with our previously reported findings that MVE-exposure promotes increased cerebral microvascular AT1 expression in C57BL/6 mice [44]. There was also an increase in vascular AT1 receptor expression in the FA + HF group at the protein level. While we did not observe elevated plasma Ang II levels in the FA + HF mice, we have previously reported that oxidized LDL (oxLDL) in plasma is upregulated in both FA + HF and MVE + HF C57BL/6 mice [45]. Crosstalk between Ang II and oxLDL,

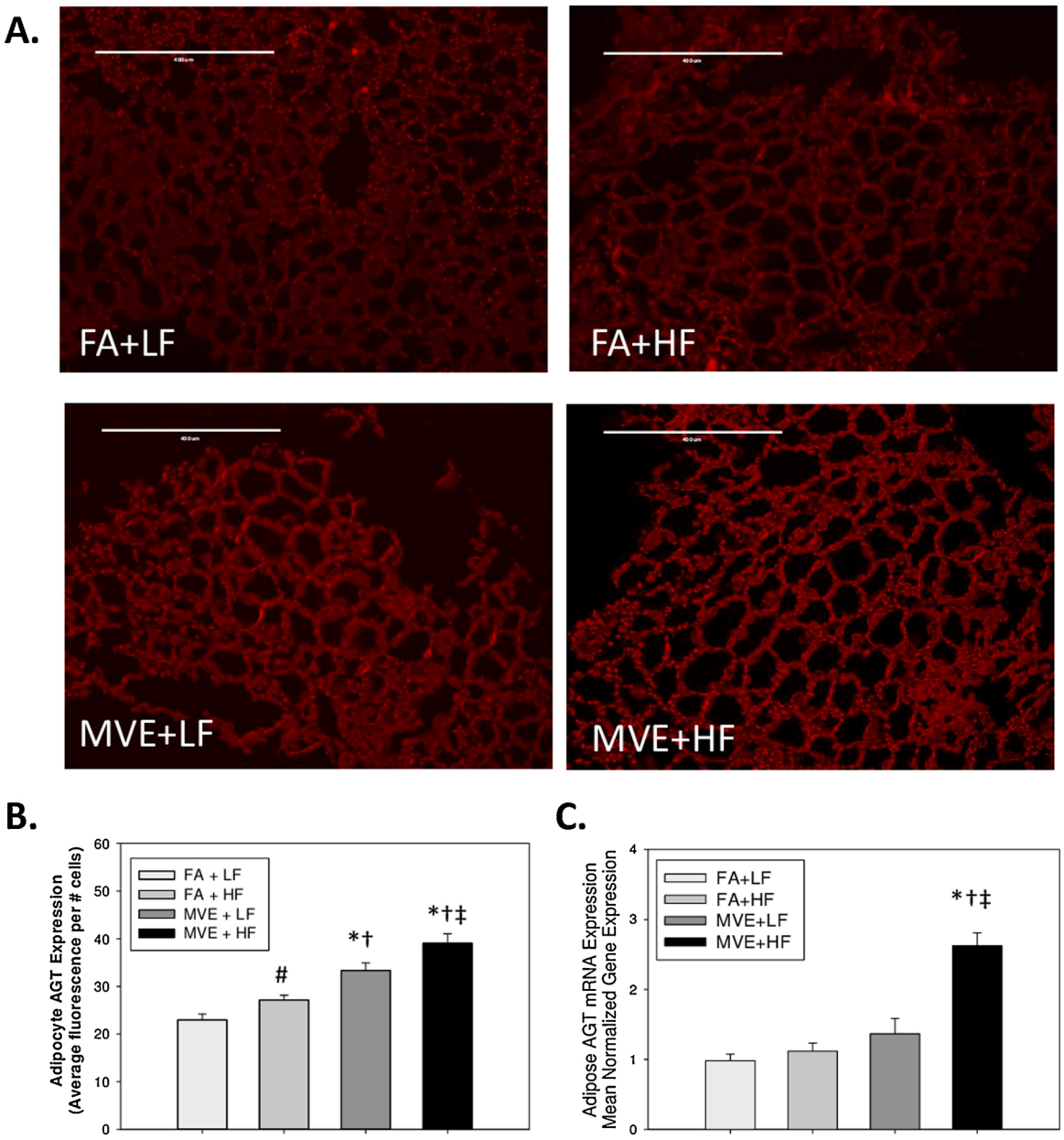

Fig. 9. Representative images of Angiotensinogen (AGT) expression (red) in the epididymal adipose tissue of male C57BL/6 mice exposed via inhalation to either filtered air (FA) while fed a low-fat (LF) diet, FA while fed a high-fat (HF) diet, 100 μg PM/m^3 of mixed vehicle emissions (MVE) while fed a LF diet or MVE while fed a HF diet. All MVE and FA control exposures were conducted for 6 h/d, 7 d/wk, for a period of 30 d. (B) Fluorescence was measured, graphed, and is shown as mean f0b1; SEM (4 sections each; n = 4 per exposure group). 10x magnification; scale bar = 400 μm. (C) Adipose AGT mRNA expression, as determined by real time RT-qPCR (n = 8). *p ≤ 0.05 compared to FA + LF; †p ≤ 0.05 compared to FA + HF; ‡p ≤ 0.05 compared to MVE + LF using a 2-way ANOVA.

and the respective receptors, has been characterized in the cardiovascular system and oxLDL shown to upregulate AT1 receptor expression via the lectin-like oxLDL receptor (LOX)-1 [69]. Such crosstalk may account for the upregulation of vascular AT1, without concurrent increases in circulating Ang II, observed in the HF + FA animals; however, further mechanistic studies are necessary to tease apart the signaling pathways from MVE exposure vs. HF diet.

Increased Ang II – AT1 signaling in the vasculature mediates multiple CVD pathologies, including atherosclerosis, through ROS production and subsequent activation of cellular inflammatory and adhesion factors [20]. In the current study, MVE-exposure induced vascular ROS (as quantified by DHE), MOMA-2 expression, and ICAM-1, regardless of diet; however, vascular ROS and ICAM-1 were further elevated in the MVE + HF animals, compared to that observed in the MVE + LF animals. There was also an increase in vascular ROS in the FA + HF group, compared to the FA + LF group, which may be correlated with increased AT1 receptor signaling. Furthermore, vascular VCAM-1 was also significantly increased with MVE-exposure, but only in those animals on a HF diet. Induction of vascular adhesion molecules, including ICAM-1 and VCAM-1, infiltration of monocytes/macrophages, and ROS production are all early makers of atherogenesis. Therefore, in our study, MVE-exposure promotes activation of pathways involved in the pathophysiology of vascular disease in an otherwise healthy animal model, further exacerbated by the consumption of a HF diet. These findings collectively suggest that traffic-generated air pollutants are a likely environmental contributor to the etiology of CVD.

Adipose tissue structure and function change with progression from a "lean" to "obese" phenotype, although this can differ amongst people depending on their metabolic state. One of the hallmark features of obesity is adipocyte hypertrophy, which is associated with adipose

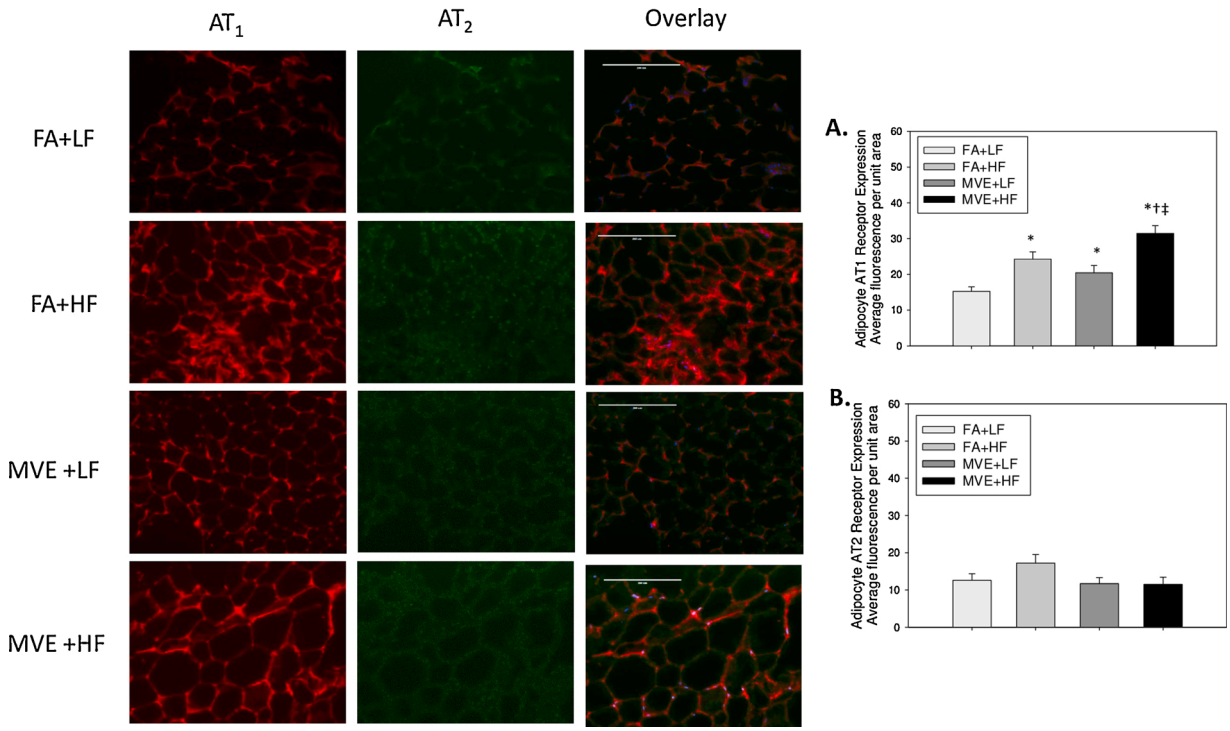

Fig. 10. Representative images of the (A) AT1 receptor (red) and (B) AT2 receptor (green) expression in the epididymal adipose tissue of male C57BL/6 mice exposed via inhalation to either filtered air (FA) while fed a low-fat (LF) diet, FA while fed a high-fat (HF) diet, 100 μg PM/m^3 of mixed vehicle emissions (MVE) while fed a LF diet or MVE while fed a HF diet. All MVE and FA control exposures were conducted for 6 h/d, 7 d/wk, for a period of 30 d (4 sections each; n = 4 per exposure group). Blue = Hoechst nuclear stain. Fluorescence was measured, graphed, and is shown as mean f0b1; SEM. 20x magnification; scale bar =200 μm. *p ≤ 0.05 compared to FA + LF; †p ≤ 0.05 compared to FA + HF; ‡p ≤ 0.05 compared to MVE + LF using a 2-way ANOVA.

tissue dysfunction, including increased macrophage infiltration, inflammation, insulin resistance, and abnormal fat storage (rev. in [70]). As expected, we see a significant increase in both body and epididymal fat pad weight in our HF diet animals than those on a LF diet. Furthermore, we observe a statistical increase in the size of adipocytes within the epididymal fat pad in our HF diet group and both MVE-exposed groups, regardless of the diet consumed. These findings indicate that MVE-exposure mediates conditions in adipose tissue that promote adipocyte hypertrophy. Additionally, we observed an increase in lipid accumulation in the adipocytes in the groups of C57BL/6 mice fed a HF diet, regardless of exposure. While visually, the MVE + HF adipose appears to have significantly more Nile Red fluorescence (e.g., lipid accumulation), even when normalized to cell count, there is such variability across HF-diet fed that a statistically significant relationship between the FA + HF vs. MVE + HF was not observed. In obesity, there is often altered lipid buffering capacity, which can lead to increased lipid accumulation in tissues other than adipose. Moreover, while adipocyte hypertrophy is observed in overweight and diabetic patients, adipocyte hyperplasia is also known to contribute to obesity [71], which was not assessed in the current study. Lipid accumulation and storage can vary significantly across different fat depots and between sexes. Further studies are necessary to characterize how exposure to inhaled traffic-generated pollutants contributes to weight gain related to adipocyte hypertrophy vs. hyperplasia and lipid storage in different tissues in both males and females.

Increased systemic and local RAS signaling can contribute to obesity and metabolic syndrome [72]. Thus, we investigated whether exposure to MVE and/or diet mediated alterations in the tissue-level adipose expression of RAS components in our mice. The epididymal adipose showed an increase in both AGT and AT1 receptors in the FA + HF, MVE + LF, and MVE + HF groups, compared to FA + LF controls, suggesting that both diet and exposure can independently mediate altered adipose RAS signaling. The MVE + HF group showed significant increases, compared to the MVE + LF and FA + HF groups, for both AGT and AT1 receptor expression; however, the combination of exposure and diet only resulted in a statistical interaction in adipose AGT expression. There was observed no change in the expression of the AT2 receptor in adipose tissue. Adipose AGT expression has been reported to be increased with obesity and contributes to inflammation and abnormal metabolic function in adipocytes [25]. Furthermore, in studies of mice with diet-induced obesity, adipose AGT levels directly correlate to circulating plasma AGT levels [73]. However, there are conflicting reports in the literature about how AGT tissue levels in adipose of obese vs. lean individuals correlate to circulating levels of AGT (rev. in [66]). Since it is a precursor to Ang II production, increased AGT expression in adipose tissue can mediate increased Ang II expression, although tissue level Ang II was not directly measured in this study. In adipose tissue, Ang II is known to signal through AT1 and AT2 receptors, which have opposing physiological roles. AT1 mediates signaling pathways associated with lipolysis, while the AT2 receptor mediates signaling pathways associated with lipogenesis (rev in. [74]). Interestingly, AT1 receptor expression has previously been reported to be upregulated in adipose tissue from obese patients with hypertension, without increased systemic RAS activation or increased tissue levels of AGT, suggesting other ligands may also signal through the AT1 receptor in these pathological states [75]. The roles of AT1 vs. AT2 receptor signaling in pro-inflammatory signaling in adipose tissue is still not fully understood, as findings from both knockout and inhibitor studies of each, individually, suggest both may contribute to inflammatory signaling in adipocytes [29,76]. Regardless, in our study, MVE-exposure mediates increased adipose AGT and AT1 expression, suggesting exposure to traffic-generated air pollution can promote signaling pathways in adipose tissue associated with pathophysiologic changes in adipocytes observed in obese individuals, further exacerbated by a HF diet.

Increased Ang II signaling in adipose tissue promotes oxidative stress, inflammation, and MCP-1 expression, as confirmed through AT1

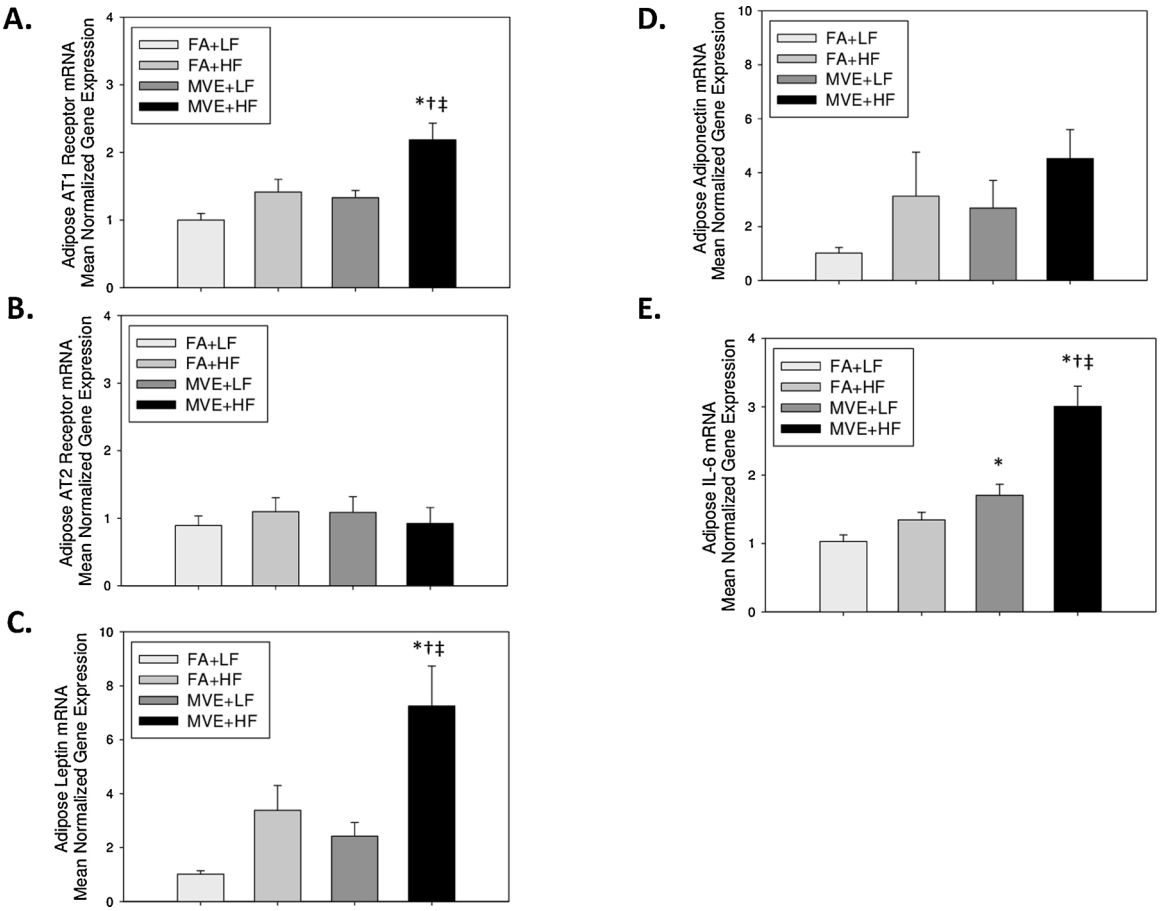

Fig. 11. Real-time RT-qPCR analyses of adipose tissue (A) AT1 Receptor, (B) AT2 receptor, (C) Leptin, (D) Adiponectin, and (E) IL-6 mRNA from male C57BL/6 mice exposed via inhalation to either filtered air (FA) while fed a low-fat (LF) diet, FA while fed a high-fat (HF) diet, 100 μg PM/m^3 of mixed vehicle emissions (MVE) while fed a LF diet or MVE while fed a HF diet. All MVE and FA control exposures were conducted for 6 h/d, 7 d/wk, for a period of 30 d. Represented as mean normalized gene expression, as calculated by $\Delta\Delta C_T$ with house-keeping gene GAPDH (n = 8 per group). *p ≤ 0.05 compared to FA + LF; †p ≤ 0.05 compared to FA + HF; ‡p ≤ 0.05 compared to MVE + LF using a 2-way ANOVA.

inhibitor studies [76,77]. Adipocyte hypertrophy is also associated with decreased adipose tissue blood flow, leading to hypoxia, and increased macrophage infiltration, inflammation, and abnormal adipokine expression [70]. The current study findings are in agreement and show that exposure to MVE promoted an increase in IL-6 mRNA expression in the adipose tissue, associated with increased MCP-1 expression, regardless of the diet consumed. Surprisingly, we did not observe a change in adipose TNF-α expression at the transcript or protein level across any study group. As macrophages are believed to be responsible for the increased production of TNF-α in adipose of obese individuals [78], it is plausible that there is a balance in the activation state of macrophages present in the adipose tissue (e.g., M1 macrophage, pro-inflammatory state vs. M2 macrophage, anti-inflammatory state) at the time point the tissues were collected for analysis. However, further time course studies are necessary to determine the exposure to macrophage accumulation initiation and the resulting pro-inflammatory signaling.

Increased inflammation, macrophage infiltration, and adipocyte expansion are also associated with metabolic disturbances, including abnormal glucose and insulin signaling. In adipose tissue, glucose is taken up via the glucose transporter, GLUT4, stimulated by insulin. The canonical insulin signaling pathway in adipocytes is initiated by activation of the IR. A hallmark feature of T2D is the inability of tissues to respond appropriately to insulin stimulation, leading to insulin resistance. We observed an increase in adipose IR-β expression in our MVE + LF group; conversely, there is a decrease in IR-β expression in our MVE + HF group at the tissue level. Decreased adipose IR-β expression has recently been associated with gestational diabetes [79], suggesting that alterations in adipose IR expression can contribute to abnormal metabolic signaling. We did not assess IR-α expression, which is a limitation of the current study; however, we chose to focus on the expression of the IR-β instead because it is known to be expressed in more differentiated adipocytes and regulates downstream expression of metabolic endpoints [57]. Adipose GLUT4 expression is reported to be downregulated in insulin-resistant obese individuals and individuals with T2D [80]. In our study, we measured a decrease in adipose GLUT4 expression in the HF + FA group, compared to the LF diet groups (regardless of exposure), with an even further decrease in expression quantified in the HF + MVE mice. These findings agree with previously published studies reporting a decrease in GLUT4 receptor expression in the adipose of mice fed a high-fat and high-carbohydrate diet [81]. Multiple GLUT4 depletion studies have shown that decreased adipose GLUT4 expression is associated with insulin resistance, a characteristic of diabetic individuals [82]. Our findings collectively suggest that MVE exposure may mediate alterations in insulin and glucose signaling in visceral adipose tissue, further exacerbated by the consumption of a HF diet.

While the current study reveals novel findings related to adipose structure and function changes resulting from inhalation exposure to traffic-generated air pollution, there are a few limitations to note. First, we characterized only one exposure duration (30 d) and concentration (100 μg PM/m^3) for the MVE exposure, and as such, our results may only be representative of subchronic exposure to reasonably high levels of pollutants. The dose and exposure duration in the current study were

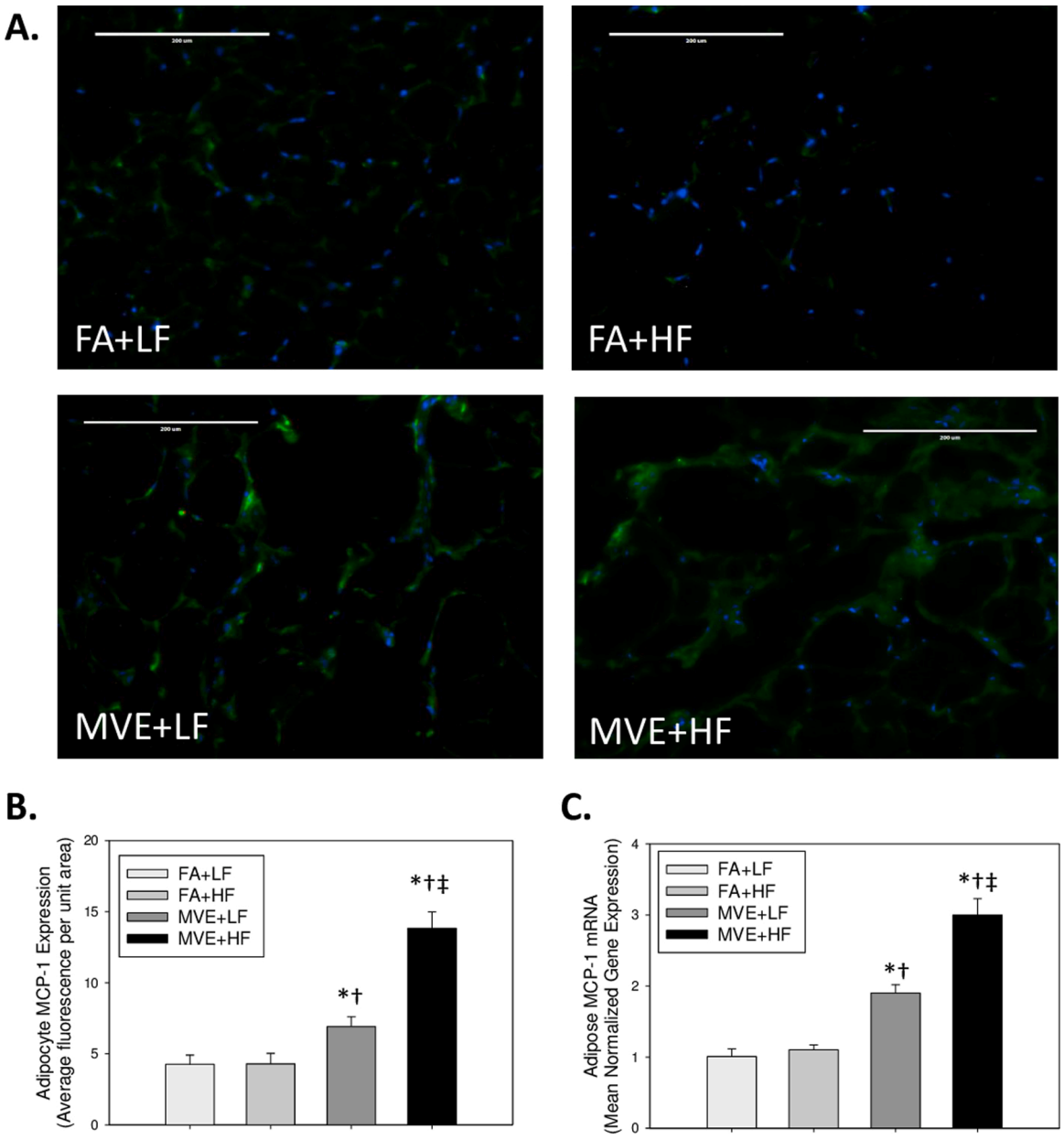

Fig. 12. Representative images of monocyte chemoattractant protein (MCP)-1 expression (green) in the epididymal adipose tissue of male C57BL/6 mice exposed via inhalation to either filtered air (FA) while fed a low-fat (LF) diet, FA while fed a high-fat (HF) diet, 100 μg PM/m^3 of mixed vehicle emissions (MVE) while fed a LF diet or MVE while fed a HF diet. All MVE and FA control exposures were conducted for 6 h/d, 7 d/wk, for a period of 30 d. (B) Fluorescence was measured, graphed, and is shown as mean f0b1; SEM (4 sections each, n = 4 per exposure group). Blue = Hoechst nuclear stain. 20x magnification; scale bar =200 μm. (C) Adipose MCP-1 mRNA expression, as determined by real time RT-qPCR (n = 8). *$p \leq 0.05$ compared to FA + LF; †$p \leq 0.05$ compared to FA + HF; ‡$p \leq 0.05$ compared to MVE + LF using a 2-way ANOVA.

utilized to compare outcomes in the kidneys, vasculature, and adipose tissue to our previously reported RAS-mediated outcomes in the cerebral microvasculature, at the same dose and MVE-exposure duration. Furthermore, while 100 μg PM/m^3 would be considered a high environmental or occupational exposure concentration, it is within $PM_{2.5}$ air pollution levels that have been recorded in multiple cities around the world in recent months [47]. It is important to note that the chemical composition of vehicle exhaust generated from the gasoline and diesel engines in the laboratory may be differ from that experienced in ambient air pollution exposures in the environment. Additionally, there can be significant variability in the composition of engine emissions related to factors other than the fuel standards, including engine type, engine load, date of manufacture of the engine, engine additives, and size and composition of the PM released, which can also account for differential toxicity outcomes related to exposure [83–85]. For example, with similar PM mass concentration, high load-related diesel engine emissions resulted in increased pulmonary inflammation and susceptibility to viral infection, while partial-load diesel engine emissions produced more pronounced effects in the cardiovascular system in $ApoE^{-/-}$ mice (e.g., elevated heart rate, altered T-wave morphology) [85]. Moreover, it is still somewhat unclear which components within the mixture vs. the mixture itself mediate toxicity in the body. Additionally, in this study, we only characterized the reported outcomes in visceral adipose tissue. Remodeling and abnormal metabolic signaling in subcutaneous adipose tissue have also been described to contribute to obesity and T2D, although changes in both morphology and metabolic function are generally correlated across these adipose depots [86]. Lastly, we only analyzed outcomes in male mice for the current study. As such, we

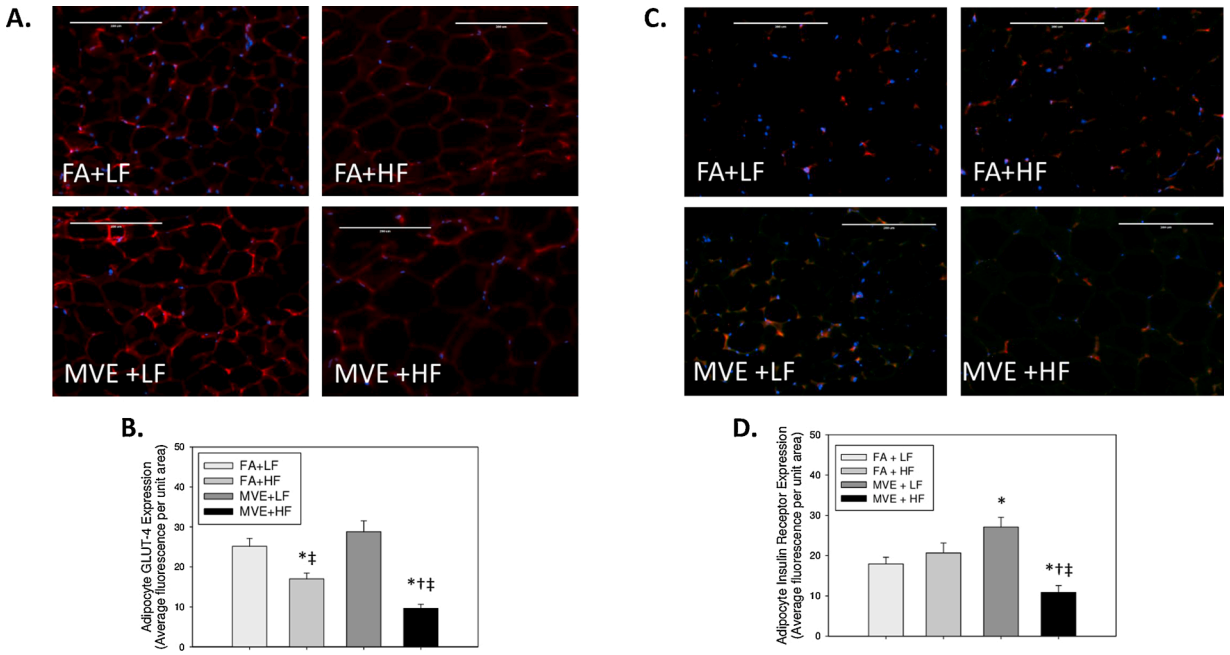

Fig. 13. Representative images of (A) glucose transporter (GLUT)-4 expression (red) in the epididymal adipose fad pad tissue of male C57BL/6 mice exposed via inhalation to either filtered air (FA) while fed a low-fat (LF) diet, FA while fed a high-fat (HF) diet, 100 μg PM/m^3 of mixed vehicle emissions (MVE) while fed a LF diet or MVE while fed a HF diet. All MVE and FA control exposures were conducted for 6 h/d, 7 d/wk, for a period of 30 d. (B) GLUT-4 fluorescence was quantified and represented as mean per number of cells f0b1; SEM (4 sections each, n = 4 per exposure group). Blue = Hoechst nuclear stain. 20x magnification; scale bar =200 μm. (C) Representative images of insulin receptor beta (IR-β) expression (red) in the epididymal adipose tissue of male C57BL/6 mice. (D) IR-β fluorescence was measured, graphed, and is shown as mean f0b1; SEM (4 sections each, n = 4 per exposure group). Blue = Hoechst nuclear stain. 20x magnification; scale bar =200 μm. *p ≤ 0.05 compared to FA + LF; †p ≤ 0.05 compared to FA + HF; ‡p ≤ 0.05 compared to MVE + LF using a 2-way ANOVA.

cannot conclude whether sexual dimorphisms might exist related to the effects of MVE exposure ± HF in females' adipose tissue.

In conclusion, our results show that subchronic traffic-generated air pollution exposure (MVE) results in elevated expression of AT1 in the systemic vasculature, which is associated with increased vascular adhesion molecule expression, monocyte/macrophage sequestration, and production of ROS, all of which are early tissue-level signaling events in the pathogenesis of CVD. Furthermore, kidney levels of renin and Ang II receptors, AT1 and AT2, were also elevated with MVE-exposure, which agrees with our previous findings of elevated plasma Ang II levels in C57BL/6 mice exposed to MVE. Correlated to the observed increase in systemic components of RAS, MVE-exposure also resulted in increased weight gain, epididymal fat pad weight, and adipocyte hypertrophy in male C57BL/6 wild-type mice that were more pronounced with consumption of a HF diet. Local adipose RAS components were also upregulated in MVE-exposed mice, including AGT and AT1 receptors. MVE-exposure was also associated with increased MCP-1, inflammation (IL-6), and leptin transcript expression, all hallmarks of an "obese" phenotype in adipose tissue. Lastly, adipose tissue from MVE-exposed animals on a HF diet also displayed decreased GLUT4 and IR-β expression, suggesting altered metabolic signaling in the adipose tissue. As CVD and obesity rates are currently increasing worldwide and are known comorbidities for other inflammatory diseases, it is essential to determine which environmental air pollutants may promote susceptibility and characterize mechanistic pathways contributing to these exposure-mediated outcomes.

Funding

These studies were supported by funding from the National Institute of Health (NIH) - National Institute of Environmental Health Sciences (NIEHS) grants R15ES026795 and R00ES016586 to A.K.L.

Disclosure statement

Funding from the National Institute of Health (NIH) - National Institute of Environmental Health Sciences (NIEHS) was used to conduct the exposures and experiments described in this manuscript.

Author contributions

B.L.P.: investigation, formal analysis, validation, writing – original draft; U.S.: investigation, formal analysis, investigation, writing – review & editing; J.L.: project administration, investigation, formal analysis, writing – review & editing; N.A.M.: formal analysis, validation, writing – review & editing; A.K.L.: conceptualization, funding acquisition, formal analysis, resources, supervision, writing – review & editing.

Declaration of Competing Interest

The authors declare that they have no known competing financial interests or personal relationships that could have appeared to influence the work reported in this paper.

Acknowledgements

We would like to thank Dr. Jacob McDonald and the Chemistry and Inhalation Exposure Group at Lovelace Respiratory Research Institute / Lovelace Biomedical Research Institute for conducting and characterizing the whole-body inhalation animal exposures.

Data is available from the corresponding author upon reasonable request.

Appendix A. Supplementary data

Supplementary material related to this article can be found, in the online version, at doi:https://doi.org/10.1016/j.toxrep.2021.04.001.

References

[1] World Health Organization (WHO), Air Pollution Overview, 2020. Accessed December 17, 2020, https://www.who.int/health-topics/air-pollution#tab=tab_1.

[2] B.A. Franklin, R. Brook, C. Arden Pope 3rd., Air pollution and cardiovascular disease, Curr. Probl. Cardiol. 40 (2015) 207–238, https://doi.org/10.1016/j.cpcardiol.2015.01.003.

[3] G. Hoek, R.M. Krishnan, R. Beelen, A. Peters, B. Ostro, B. Brunekreef, J. D. Kaufman, Long-term air pollution exposure and cardio-respiratory mortality: a review, Environ. Health 12 (2013) 43, https://doi.org/10.1186/1476-069X-12-43.

[4] American Heart Association, Heart Disease and Stroke Statistical Update Fact Sheet At-a-Glance, 2020. Accessed June 17, 2020, https://www.professional.heart.org/idc/groups/ahamah-public/@wcm/@sop/@smd/documents/downloadable/ucm_505473.pdf.

[5] M.J. Davies, N. Woolf, P.M. Rowles, J. Pepper, Morphology of the endothelium over atherosclerotic plaques in human coronary arteries, Br. Heart J. 60 (1988) 459–464, https://doi.org/10.1136/hrt.60.6.459.

[6] Y. Nakashima, E.W. Raines, A.S. Plump, J.L. Breslow, R. Ross, Upregulation of VCAM-1 and ICAM-1 at atherosclerotic-prone sites on the endothelium in the ApoE-deficient mouse, Arterioscler. Thromb. Vasc. Biol. 18 (1998) 842–851, https://doi.org/10.1161/01.ATV.18.5.842.

[7] P. Marchio, S. Guerra-Ojeda, J.M. Vila, M. Aldasoro, V.M. Victor, M.D. Mauricio, Targeting early atherosclerosis: a focus on oxidative stress and inflammation, Oxid. Med. Cell. Longev. 2019 (2019), 8563845, https://doi.org/10.1155/2019/8563845.

[8] M.A. Cornier, D. Dabelea, T.L. Hernandez, R.C. Lindstrom, A.J. Steig, N.R. Stob, R. E. Van Pelt, H. Wang, R.H. Eckel, The metabolic syndrome, Endocr. Rev. 29 (2008) 777–822.

[9] P.M. Clifton, J.B. Keogh, A systematic review of the effect of dietary saturated and polyunsaturated fat on heart disease, Nutr. Metab. Cardiovasc. Dis. 27 (2017) 1060–1080.

[10] Y. Wang, F. Wang, J. Yuan, J. Li, D. Jiang, J. Zhang, H. Li, R. Wang, J. Tang, T. Z. Huang, et al., Effects of dietary fat on gut microbiota and faecal metabolites, and their relationship with cardiometabolic risk factors: a 6-month randomized controlled-feeding trial, Gut. 68 (2019) 1417–1429, https://doi.org/10.1136/gutjnl-2018-317609.

[11] R. Ghosh, F. Lurmann, L. Perez, B. Penfold, S. Brandt, J. Wilson, M. Milet, N. Künzli, R. McConnel, Near-roadway air pollution and coronary heart disease: burden of disease and potential impact of greenhouse gas reduction strategy in Southern California, Environ. Health Perspect. 124 (2016) 196–200, https://doi.org/10.1289/ehp.1408865.

[12] S. Jiang, L. Bo, C. Gong, X. Du, H. Kan, Y. Xie, W. Song, J. Zhao, Traffic-related air pollution is associated with cardio-metabolic biomarkers in general residents, Int. Arch. Occup. Environ. Health 89 (2016) 911–921, https://doi.org/10.1001/jama.294.23.3003.

[13] M.R. Miller, S.G. McLean, R. Duffin, A.O. Lawal, J.A. Araujo, C.A. Shaw, N.L. Mills, K. Donaldson, D.E. Newby, P.W. Hadoke, Diesel exhaust particulate increases the size and complexity of lesions in atherosclerotic mice, Part. Fibre Toxicol. 10 (2013) 61, https://doi.org/10.1186/1743-8977-10-61.

[14] K. Wolf, A. Popp, A. Schneider, S. Breitner, R. Hampel, W. Rathmann, C. Herder, M. Roden, W. Koenig, C. Meisinger, A. Peters, KORA-Study Group, Association between long-term exposure to air pollution and biomarkers related to insulin resistance, subclinical inflammation, and adipokines, Diabetes. 65 (2016) 3314–3326, https://doi.org/10.2337/db15-1567.

[15] W. Li, K.S. Dorans, E.H. Wilker, M.B. Rice, J. Schwartz, B.A. Coull, P. Koutrakis, D. R. Gold, C.S. Fox, M.A. Mittleman, Residential proximity to major roadways, fine particulate matter, and adiposity: the Framingham Heart Study, Obesity (Silver Spring) 24 (2016) 2593–2599, https://doi.org/10.1002/oby.21630.

[16] X. Zhang, H. Zhao, W.H. Chow, M. Bixby, C. Durand, C. Markham, K. Zhang, Population-Based Study of traffic-related air pollution and obesity in Mexican Americans, Obesity (Silver Spring) 28 (2020) 412–420, https://doi.org/10.1002/oby.22697.

[17] Y. Wei, J.J. Zhang, Z. Li, A. Gow, K.F. Chung, M. Hu, Z. Sun, L. Zeng, T. Zhu, G. Jia, et al., Chronic exposure to air pollution particles increases the risk of obesity and metabolic syndrome: findings from a natural experiment in Beijing, FASEB J. 30 (2016) 2115–2122, https://doi.org/10.1096/fj.201500142.

[18] H. Castrop, K. Hocherl, A. Kurtz, F. Schweda, V. Todorov, C. Wagner, Physiology of kidney renin, Physiol. Rev. 90 (2010) 607–673, https://doi.org/10.1152/physrev.00011.2009.

[19] R.E. Schmieder, K.F. Hilgers, M.P. Schlaich, B.M. Schmidt, Renin angiotensin system and cardiovascular risk, Lancet 369 (2007) 1208–1219, https://doi.org/10.1016/S0140-6736(07)60242-6.

[20] A.M. Garrido, K.K. Griendling, NADPH oxidases and angiotensin II receptor signaling, Mol. Cell. Endocrinol. 302 (2009) 148–158, https://doi.org/10.1016/j.mce.2008.11.003.

[21] C. Tai, T. Gan, L. Zou, Y. Sun, Y. Zhang, W. Chen, J. Li, J. Zhang, Y. Xu, L. Huihe, et al., Effect of angiotensin-converting enzyme inhibitors and angiotensin II receptor blockers on cardiovascular events in patients with heart failure: a meta-analysis of randomized controlled trials, BMC Cardiovasc. Disord. 17 (2017) 257, https://doi.org/10.1186/s12872-017-0686-z.

[22] K. Pan, S. Jiang, X. Du, X. Zeng, J. Zhang, L. Song, L. Lei, J. Zhou, H. Kan, Q. Sun, Y. Xie, C. Dong, J. Zhao, Parental $PM_{2.5}$ exposure changes Th17/Treg cells in offspring, is associated with elevation of blood pressure, Environ. Toxicol. (Febuary 19) (2021), https://doi.org/10.1002/tox.23114. Online ahead of print.

[23] M. Paul, A. Poyan Mehr, R. Kreutz, Physiology of local renin angiotensin systems, Physiol. Rev. 86 (2006) 747–803, https://doi.org/10.1152/physrev.00036.2005.

[24] S. Engeli, J. Bohnke, K. Gorzelniak, J. Janke, P. Schling, M. Bader, F.C. Luft, A. M. Sharma, Weight loss and the renin-angiotensin-aldosterone system, Hypertension. 45 (2005) 356–362, https://doi.org/10.1161/01.HYP.0000154361.47683.d3.

[25] F. Massiera, J. Seydoux, A. Geloen, A. Quignard-Boulange, S. Turban, P. Saint-Marc, A. Fukamizu, R. Negrel, G. Ailhaud, M. Teboul, Angiotensinogen-deficient mice exhibit impairment of diet-induced weight gain with alteration in adipose tissue development and increased locomotor activity, Endocrinology 142 (2001) 5220–5225, https://doi.org/10.1210/endo.142.12.8556.

[26] A.P. Jayasooriya, M.L. Mathai, L.L. Walker, D.P. Begg, D.A. Denton, D. Cameron-Smith, G.F. Egan, M.J. McKinley, P.D. Rodger, A.J. Sinclair, et al., Mice lacking angiotensin-converting enzyme have increased energy expenditure, with reduced fat mass and improved glucose clearance, Proc. Natl. Acad. Sci. U.S.A. 105 (2008) 6531–6536, https://doi.org/10.1073/pnas.0802690105.

[27] J.A. Saye, L.A. Cassis, T.W. Sturgill, K.R. Lynch, M.J. Peach, Angiotensinogen gene expression in 3T3-L1 cells, Am. J. Physiol. 256 (1989) C448–C451, https://doi.org/10.1152/ajpcell.1989.256.2.C448.

[28] N. Takahashi, F. Li, K. Hua, J. Deng, C.H. Wang, R.R. Bowers, T.J. Bartness, H. S. Kim, J.B. Harp, Increased energy expenditure, dietary fat wasting, and resistance to diet-induced obesity in mice lacking renin, Cell Metab. 6 (2007) 506–512, https://doi.org/10.1016/j.cmet.2007.10.011.

[29] L. Yvan-Charvet, P. Even, M. Bloch-Faure, M. Guerre-Millo, N. Moustaid-Moussa, P. Ferre, A. Quignard-Boulangé, Deletion of the angiotensin type 2 receptor (AT2R) reduces adipose cell size and protects from diet-induced obesity and insulin resistance, Diabetes. 54 (2005) 991–999, https://doi.org/10.2337/diabetes.54.4.991.

[30] P.M. Smith, C.C. Hindmarch, D. Murphy, A.V. Ferguson, AT1 receptor blockade alters nutritional and biometric development in obesity-resistant and obesity-prone rats submitted to a high fat diet, Front. Psychol. 5 (2014) 832, https://doi.org/10.3389/fpsyg.2014.00832.

[31] Y. Tomono, M. Iwai, S. Inaba, M. Mogi, M. Horiuchi, Blockade of AT1 receptor improves adipocyte differentiation in atherosclerotic and diabetic models, Am. J. Hypertens. 21 (2008) 206–212, https://doi.org/10.1038/ajh.2007.50.

[32] Y. Wei, J.R. Sowers, R. Nistala, H. Gong, G.M. Uptergrove, S.E. Clark, E.M. Morris, N. Szary, C. Manrique, C.S. Stump, Angiotensin II-induced NADPH oxidase activation impairs insulin signaling in skeletal muscle cells, J. Biol. Chem. 281 (2006) 35137–35146, https://doi.org/10.1074/jbc.M601320200.

[33] T. Ogihara, T. Asano, K. Ando, Y. Chiba, H. Sakoda, M. Anai, N. Shojima, H. Ono, Y. Onishi, M. Fujishiro, et al., Angiotensin II-induced insulin resistance is associated with enhanced insulin signaling, Hypertension. 40 (2002) 872–879, https://doi.org/10.1161/01.hyp.0000040262.48405.a8.

[34] X. Chen, S.L. Zhang, L. Pang, J.G. Filep, S.S. Tang, J.R. Ingelfinger, J.S. Chan, Characterization of a putative insulin-responsive element and its binding protein(s) in rat angiotensinogen gene promoter: regulation by glucose and insulin, Endocrinology. 142 (2001) 2577–2585, https://doi.org/10.1210/endo.142.6.8214.

[35] A.R. Brasier, J. Li, Mechanisms for inducible control of angiotensinogen gene transcription, Hypertension. 27 (1996) 465–475, https://doi.org/10.1161/01.hyp.27.3.465.

[36] B. Wang, J.R. Jenkins, P. Trayhurn, Expression and secretion of inflammation related adipokines by human adipocytes differentiated in culture: integrated response to TNF-alpha, Am. J. Physiol. Endocrinol. Metab. 288 (2005) E731–E740, https://doi.org/10.1152/ajpendo.00475.2004.

[37] G.S. Hotamisligil, Inflammatory pathways and insulin action, Int. J. Obes. 27 (2003) S53–S55, https://doi.org/10.1038/sj.ijo.0802502.

[38] S. Asamizu, M. Urakaze, C. Kobashi, M. Ishiki, A.K. Norel Din, S. Fujisaka, Y. Kanatani, A. Bukahari, S. Senda, H. Suzuki, et al., Angiotensin II enhances the increase in monocyte chemoattractant protein-1 production induced by tumor necrosis factor-{alpha} from 3T3-L1 preadipocytes, J. Endocrinol. 202 (2009) 199–205, https://doi.org/10.1677/JOE-08-0363.

[39] T. Skurk, V. van Harmelen, H. Hauner, Angiotensin II stimulates the release of interleukin-6 and interleukin-8 from cultured human adipocytes by activation of NF-kappaB, Arterioscler. Thromb. Vasc. Biol. 24 (2004) 1199–1203, https://doi.org/10.1161/01.ATV.0000131266.38312.2e.

[40] M. Borro, P. Di Girolamo, G. Gentile, O. De Luca, R. Preissner, A. Marcolongo, S. Ferracuti, M. Simmaco, Evidence-based considerations exploring relations between SARS-COV-2 pandemic and air pollution: involvement of PM2.5-mediated up-regulation of the viral receptor ACE-2, In J Environ Res Public Health. 17 (2020) 5573, https://doi.org/10.3390/ijerph17155573.

[41] M. Gallo, M.E. Street, F. Guerra, V. Fanos, M.A. Marcialis, A review of current knowledge on pollution, cigarette smoling and COVID-19 diffusion and their relationship with inflammation, Acta Biomed. 91 (2020), e2020148, https://doi.org/10.23750/abm.v91i4.10263.

[42] M. Alifano, P. Alifano, P. Forgez, A. Iannelli, Renin-angiotensin system at the heart of COVID-19 pandemic, Biochimie 174 (2020) 30–33, https://doi.org/10.1016/j.biochi.2020.04.008.

[43] V. Tanwar, J.M. Adelstein, L.E. Wold, Double trouble: combined cardiovascular effects of particulate matter exposure and coronavirus disease 2019, Cardiovasc. Res. (117) (2021) 85–95, https://doi.org/10.1093/cvr/cvaa293.

[44] U. Suwannasual, J. Lucero, G. Davis, J.D. Mcdonald, A.K. Lund, Mixed vehicle emissions induces angiotensin II and cerebral microvascular angiotensin receptor expression in C57BL/6 mice and promotes alterations in integrity in a blood-brain barrier coculture model, Toxicol. Sci. 170 (2019) 525–535, https://doi.org/10.1016/j.envres.2017.10.029.

[45] U. Suwannasual, J. Lucero, J.D. McDonald, A.K. Lund, Exposure to traffic-generated air pollutant mediates alterations in brain microvascular integrity in

wildtype mice on a high fat diet, Environ. Res. 160 (2018) 449–461, https://doi.org/10.1016/j.envres.2017.10.029.
[46] L.G. Costa, T.B. Cole, J. Coburn, Y.-C. Chang, K. Dao, P.J. Roqué, Neuortoxicity of traffic-related air pollution, Neurotoxicity. 59 (2017) 133–139, https://doi.org/10.1016/j.neuro.2015.11.008.
[47] IQAir, World's Most Polluted Cities, 2019 (PM2.5). https://www.iqair.com/world-most-polluted-cities?continent=&country=&state=&page=1&perPage=50&cities=. Accessed July 9, 2020.
[48] A. Pronk, J. Coble, P. Stewart, Occupational exposure to diesel engine exhaust: a literature review, J. Expo. Sci. Environ. Epidemiol. 19 (2009) 443–457, https://doi.org/10.1038/jes.2009.21.
[49] M.J. Campen, A.K. Lund, T.L. Knuckles, D.J. Conklin, B. Bishop, D. Young, S. Seilkop, J.C. Seagrave, M.D. Reed, J.D. McDonald, Inhaled diesel emissions alter atherosclerotic plaque composition in ApoE$^{-/-}$ mice, Toxicol. Appl. Pharmacol. 242 (2010) 310, https://doi.org/10.1016/j.taap.2009.10.021.
[50] A.K. Lund, J. Lucero, M. Harman, M.C. Madden, J.D. McDonald, J.C. Searave, M. J. Campen, The oxidized low density lipoprotein receptor mediates vascular effects of inhaled vehicle emissions, Am. J. Respir. Crit. Care Med. (184) (2011) 82–89, https://doi.org/10.1186/1743-8977-10-62.
[51] A.K. Lund, J. Lucero, S. Lucas, M.C. Madden, J.D. McDonald, J.C. Seagrave, T. L. Knuckles, M.J. Campen, Vehicular emissions induce vascular MMP-9 expression and activity associated with vascular endothelin-1 mediated pathways, Arterioscler. Thromb. Vasc. Biol. 29 (2009) 511–517, https://doi.org/10.1161/ATVBAHA.108.176107.
[52] H.A. Oppenheim, J. Lucero, A.-C. Guyot, L.M. Herbert, J.D. McDonald, A. Mabondzo, A.K. Lund, Exposure to vehicle emissions results in altered blood brain barrier permeability and expression of matrix metalloproteinases and tight junction proteins in mice, Part. Fibre Toxicol. 10 (62) (2013), https://doi.org/10.1186/1743-8977-10-62 doi: 10.1073/pnas.0409451102.
[53] F. Asamizu, M. Bloch-Faure, D. Ceiler, K. Murakami, A. Fukamizu, J.M. Gasc, A. Quignard-Boulange, R. Negrel, G. Ailhaud, et al., Adipose angiotensinogen is involved in adipose tissue growth and blood pressure regulation, FASEB J. 15 (2001) 2727–2729, https://doi.org/10.1096/fj.01-0457fje.
[54] P.A. Kern, G. Di Gregorio, T. Lu, N. Rassouli, G. Ranganathan, Perilipin expression in human adipose tissue is elevated with obesity, J. Clin. Endocrinol. Metab. 89 (2004) 1352–1358, https://doi.org/10.1210/jc.2003-031388.
[55] S. Kouidhi, R. Berrhouma, K. Rouissi, S. Jarboui, M.S. Clerget-Froidevaux, I. Seugnet, F. Bchir, B. Demeneix, H. Guissouma, A.B. Elgaaied, Human subcutaneous adipose tissue Glut 4 mRNA expression in obesity and type 2 diabetes, Acta Diabetol. 50 (2013) 227–232.
[56] P.M. Moraes, A. Saghatelian, B.B. Kahn, Glut 4 expression in adipocytes regulates de novo lipogenesis and levels of a novel class of lipids with antidiabetic and anti-inflammatory effects, Diabetes 65 (2016) 1808–1815, https://doi.org/10.2337/db16-0221.
[57] A. Cignarelli, V.A. Genchi, S. Perrini, A. Natalicchio, L. Laviola, F. Giorgina, Insulin and insulin receptors in adipose tissue development, Int. J. Mol. Sci. 20 (2019) 759, https://doi.org/10.3390/ijms20030759.
[58] E.J. Benjamin, P. Muntner, A. Alonso, M.S. Bittencourt, C.W. Callaway, A. P. Carson, A.M. Chamberlain, A.R. Chang, S. Cheng, S.R. Das, F.N. Delling, et al., Heart disease and stroke statistics – 2019 update: a report from the American Heart Association, Circulation (139) (2019) e56–e528, https://doi.org/10.1161/CIR.0000000000000659.
[59] T.A. Barroso, L.B. Marins, R. Alves, A.C.S. Gonçalves, S.G. Barroso, G.D.S. Rocha, Association of central obesity with the incidence of cardiovascular diseases and risk factors, Int J Cardiovasc Sci. 30 (2017) 5, https://doi.org/10.5935/2359-4802.20170073.
[60] P. Brochu, M. Bouchard, S. Haddad, Physiological daily inhalation rates for health risk assessment in overweight/obese children, adults, and elderly, Risk Anal. 34 (2014) 567–582, https://doi.org/10.1111/risa.12125.
[61] World Health Organization (WHO), Obesity and Overweight, 2020. Accessed December 19, 2020, https://www.who.int/news-room/fact-sheets/detail/obesity-and-overweight.
[62] R. An, M. Ji, H. Yan, C. Guan, Impact of ambient air pollution on obesity: a systemic review, Int. J. Obes. 42 (2018) 1112–1126, https://doi.org/10.1038/s41366-018-0089-y.
[63] J. de Bont, M. Casas, J. Barrera-Gómez, M. Cirach, I. Rivas, D. Valvi, M. Álvarez, P. Dadvand, J. Sunyer, M. Vrijheid, Ambient air pollution and overweight and obesity in school-aged children in Barcelona, Spain. Environ Int. 125 (2019) 58–64, https://doi.org/10.1016/j.envint.2019.01.048.
[64] M. Vrijheid, S. Fossati, L. Maitre, S. Márquez, T. Roumeliotaki, L. Agier, S. Andrusaityte, S. Cadiou, M. Casas, M. de Castro, et al., Early-life environmental exposures and childhood obesity: an exposome-wide approach, Environ. Health Perspect. 128 (2020) 67009, https://doi.org/10.1289/EHP5975.
[65] A.C. Montezano, A.N.D. Cat, F.J. Rios, R.M. Touyz, Angiotensin II and vascular injury, Curr. Hypertens. Rep. 16 (2014) 431, https://doi.org/10.1007/s11906-014-0431-2.
[66] M.T.J. Schütten, Houben AJHM, P.W. de Leeuw, C.D.A. Stehouwer, The Link Between Adipose Tissue Renin-angiotensin-Aldosterone System Signaling and Obesity-associated Hypertension., 2017, pp. 197–209, https://doi.org/10.1152/physiol.00037.2016, 32.
[67] S.J. Forrester, G.W. Booz, C.D. Sigmund, T.M. Coffman, T. Kawai, V. Rizzo, R. Scalia, S. Eguchi, Angiotensin II signal transduction: an update on mechanism of physiology and pathophysiology, Physiol. Rev. 98 (2018) 1627–1738, https://doi.org/10.1152/physrev.00038.2017.
[68] I. Stroo, N. Claessen, G.J.D. Teske, L.M. Butter, S. Florquin, J.C. Leemans, Deficiency for the chemokine monocyte chemoattractant protein-1 aggravates tubular damage after renal ischemia/reperfusion injury, PLoS One 10 (2015), https://doi.org/10.1371/journal.pone.0123203.
[69] D. Wei, T. Saldeen, F. Romer, J.L. Mehta, Oxidized LDL upregulates angiotensin II type 1 receptor expression in cultured human coronary artery endothelial cells: the potential role of transcription factor NF-kappaβ, Circulation 102 (2000) 1970–1976, https://doi.org/10.1007/s10557-011-6331-7.
[70] G.H. Goossens, The role of adipose tissue dysfunction in the pathogenesis of obesity-related insulin resistance, Physiol. Behav. 94 (2008) 206–218, https://doi.org/10.1016/j.physbeh.2007.10.010.
[71] L.A. Muir, C.K. Neeley, A.M. Meyer, N.A. Baker, A.M. Brosius, A.R. Washabaugh, O. A. Varban, J.F. Finks, B.F. Zamarron, C.G. Flesher, J.S. Chang, J.B. DelProposto, L. Geletka, G. Martinez-Santibanez, N. Kaciroti, C.N. Lemeng, R.W. O'Rourke, Adipose tissue fibrosis, hypertrophy, and hyperplasia: correlations with diabetes in human obesity, Obesity (Silver Spring) 24 (2016) 597–605, https://doi.org/10.1002/oby.21377.
[72] N.K. Littlejohn, J.L. Grobe, Opposing tissue-specific roles of angiotensin in the pathogenesis of obesity, and implications for obesity-related hypertension, Am. J. Physiol. Regul. Integr. Comp. Physiol. 309 (2015) R1463–R1473, https://doi.org/10.1152/ajpregu.00224.2015.
[73] S. Yasue, H. Masuzaki, S. Okada, T. Ishii, C. Kozuka, T. Tanaka, J. Fujikura, K. Ebihara, K. Hosoda, A. Katsurada, et al., Adipose tissue specific regulation of angiotensinogen in obese humans and mice: impact of nutritional status and adipocyte hypertrophy, Am. J. Hypertens. 23 (2010) 425–431, https://doi.org/10.1038/ajh.2009.263.
[74] L. Yvan-Charvet, A. Quignard-Boulangé, Role of adipose tissue renin-angiotensin system in metabolic and inflammatory diseases associated with obesity, Kid Int. 79 (2011) 162–168, https://doi.org/10.1038/ki.2010.391.
[75] E. Faloia, C. Gatti, M.A. Camilloni, B. Mariniello, C. Sardu, G.G.M. Garrapa, F. Mantero, Giacchetti, Comparison of circulting and local adipose tissue renin-angiotensin system in normotensive and hypertensive obese patients, J. Endocrinol. Invest. 25 (2002) 309–314, https://doi.org/10.1007/BF03344010.
[76] A. Kurata, H. Nishizwa, S. Kihara, N. Maeda, M. Sonoda, T. Okada, K. Ohashi, T. Hibuse, K. Fujita, A. Yasui, et al., Blockade of angiotensin II type-1 receptor reduces oxidative stress in adipose tissue and ameliorates adipocytokine dysregulation, Kidney Int. 70 (2006) 1717–1724, https://doi.org/10.1038/sj.ki.5001810.
[77] K. Tsuchiya, T. Yoshimoto, Y. Hirono, T. Tateno, T. Sugiyama, Y. Hirata, Angiotensin II induces monocyte chemoattractant protein-1 expression via a nuclear factor-kappaB-dependent pathway in rat preadipocytes, Am. J. Physiol. Endocrinol. Metab. 291 (2006) E771–E778, https://doi.org/10.1152/ajpendo.00560.2005.
[78] S. Weisberg, D. McCann, M. Desai, M. Rosenbaum, Leibel Rl, A.W. Ferrante Jr., Obesity is associated with macrophage accumulation in the adipose tissue, J. Clin. Invest. 112 (2003) 1796–1808, https://doi.org/10.1172/JCI19246.
[79] R. Ott, K. Melchior, J.H. Stupin, T. Ziska, K. Schellong, W. Henrich, R.C. Rancourt, Plagemann, Reduced insulin recenptor expression and altered DNA methylation in fat tissues and blood of women with GDM and offspring, J. Clin. Endocrinol. Metab. 104 (2019) 137–149, https://doi.org/10.1210/jc.2018-01659.
[80] E. Carvalho, Insulin resistance with low cellular IRS-1 expression is also associated with low GLUT4 expression and impaired insulin-stimulated glucose transport, FASEB J. 15 (2001) 1101–1103, https://doi.org/10.1096/fj.00-0435fje.
[81] W. Oh, L.A. Abu-Elheiga, P. Kordari, Z. Gu, T. Shaikenov, S.S. Chirala, S.J. Wakil, Glucose and fat metabolism in adipose tissue of acetyl-CoA carboxylase 2 knockout mice, Proc. Natl. Acad. Sci. U.S.A. 102 (2005) 1384–1389.
[82] E.D. Abel, O. Peroni, J.K. Kim, Y.B. Kim, O. Boss, E. Hardo, T. Minnemann, G. I. Shulman, B.B. Kahn, Adipose-selective targeting of the GLUT4 gene impairs insulin action in the muscle and liver, Nature 409 (2001) 729–733, https://doi.org/10.1038/35055575.
[83] V.V. Chernyshev, A.M. Zakharenko, S.M. Ugay, T.T. Hien, L.H. Hai, S.M. Olesik, A. S. Kholodov, E. Zubko, M. Kokkinakis, T.I. Burykina, A.K. Stratidakis, Y. O. Mezhuez, D.A. Sarigiannis, A. Tsatsakis, K.S. Golokhvast, Morphological and chemical composition of particulate matter in buses exhaust, Toxicol. Rep. 6 (2018) 120–125, https://doi.org/10.1016/j.toxrep.2018.12.002.
[84] K.S. Golokhvast, V.V. Chernyshev, V.V. Chaika, S.M. Ugay, E.V. Zelinskaya, Tsatsakis Am, S.P. Karakitsios, D.A. Sarigiannis, Size-segregated emissions and metal content of vehicle-emitted particles as a function of mileage: implications to population exposure, Environ. Res. 142 (2015) 479–485, https://doi.org/10.1016/j.envres.2015.07.018.
[85] J.D. McDonald, M.J. Campen, K.S. Harrod, J.C. Seagrave, S.K. Seilkop, J. L. Mauderly, Engine-operating load influences diesel exhaust composition and cardiopulmonary and immune responses, Environ. Health Perspect. 119 (2011) 1136–1141, https://doi.org/10.1289/ehp.1003101.
[86] A. Belligoli, C. Compagnin, M. Sanna, F. Favaretto, R. Fabris, L. Busetto, M. Foletto, C. Dal Prá, L. Prevedello, C. Da Re, et al., Characterization of subcutaneous and omental adipose tissue in patients with obesity and with different degrees of glucose impairment, Sci. Rep. 9 (2019) 11333, https://doi.org/10.1038/s41598-019-47719-y.